Interactions of Glucose Supply, AMPK and the mTOR Pathway During Early in Vitro Human Neurogenesis

Shaan Baig
Keble College

A thesis submitted for the degree of
MSc (by research) Clinical Neurosciences
Michaelmas 2023

Table of Contents

Acknowledgments: *4*

Abstract: *5*

Introduction: *7*

Neuroepithelial sheet formation 7

Glucose and AMPK signalling 7

mTOR pathway 8

Tuberous sclerosis complex 2 (TSC2) 9

Metabolic pathways during neurogenesis 11

In vitro models to recapitulate neurogenesis 13

Specific Aims 14

Methods *15*

Human embryonic stem cell lines 15

Human embryonic stem cell line maintenance and passaging 15

Neuronal differentiation from TSC2 +/+ and TSC2 -/- 15

Metformin treatment 16

Immunocytochemistry 16

RNA Extraction 17

Determination of gene expression 17

ATP assay 18

Western Blotting 19

Statistical Analysis 20

Results *21*

Confirmation of neuroepithelial sheet formation 21

Energy status is stable in early neurogenesis in wildtype cells irrespective of glucose supply 23

Hyperglycaemia alters mTORC1 dynamics associated with differentiation to neuroepithelium 24

Metformin effects are dependent on glucose supply and differentiation time-point 25

Loss of TSC2 results in dysregulated energy status during early neurogenesis 27

Glucose supply but not metformin affects mTOR activity in the absence of TSC2 during early neurogenesis 30

Discussion *32*

Limitations 38

Future directions 38

Conclusions 39

References *40*

Appendix: 54

Acknowledgments:

I am sincerely grateful to my supervisor Professor Zameel Cader who has provided guidance for the duration of my degree and feedback on presentations, data and written reports. I am especially grateful to my day-to-day supervisor, Dr. Tanya Singh for the endless support I received throughout my project, and advice on building critical skills to navigate graduate school. I would also like to acknowledge my lab mate Florian Zirpel who was alongside me for my time in the Molecular Translational Neuroscience Group, always available to talk through ideas. I would also like to thank the Masason Foundation for which their generous support has allowed me to study at the University of Oxford. Lastly, I would like to thank my family who have been a constant anchor and support in pursing my ambitions.

Abstract:

Background: Neurogenesis requires orchestration of energy status and metabolism. The AMPK pathway which feeds into the mTOR pathway, is activated upon a reduced ratio of ATP to AMP, and through altering metabolic balance, can restore ATP levels (Xiao et al., 2011). Glucose has been reported to have potent effects on AMPK and mTOR, with TSC2 as a key intermediary (Huynh et al., 2023). However, previous experiments have largely been undertaken in immortalised cell lines and the physiological relevance is therefore unclear.

Aims: The goal was to understand how glucose supply affects energy status and mTOR pathway activity during early neurogenesis.

Methods: Isogenic human embryonic stem (ES) cells with or without a TSC2 gene deletion were differentiated into neuroepithelial sheets as first described by Shi et al. (2012) under high glucose [25mM] or physiological glucose [5mM] conditions for 12 days. ATP levels, AMPK activation and mTOR activation were measured over differentiation time.

Results: ATP levels significantly increased over time, irrespective of media glucose levels in wildtype ES cells differentiated to neuroepithelium ($p<0.001$**).** In contrast, AMPK activity was stable regardless of glucose supply or time-point. mTORC1 activity significantly reduced as differentiation progressed, peaking at Day 1 in 5mM glucose and at Day 6 in 25mM glucose ($p<0.0001$**),** Metformin, an AMPK activator, had no effect on ATP levels or AMPK activation in either condition.

ATP levels decreased in TSC2 -/- compared to TSC2 +/+ cells in both glucose conditions. mTORC1 activity in TSC2 -/- significantly increased as differentiation progressed ($p<0.0001$**)**, where activity was significantly reduced in hyperglycaemic conditions. Metformin reversed

the very high AMPK activity at Day 12 in TSC2-/- cells, while having no effect on mTORC1 activity at any time-point.

Findings: Wildtype cells appeared to have stable ATP levels and AMPK activity irrespective of altered glucose supply. However, a shift in mTORC1 dynamics during early neuronal differentiation was evident. Cells without TSC2 present with dysregulated AMPK in physiological relevant conditions and significantly suppressed mTORC1 activity when cells are in hyperglycaemic conditions. The lack of effect of metformin may represent different pathways which are employed to generate ATP in the early stages of neurogenesis.

Introduction:

Neuroepithelial sheet formation

Neurogenesis is the intricate process through which pluripotent cells of the embryo are directed to form structures of the central nervous system. The process begins with neurulation, the formation of the neuroepithelial sheet arising from the ectoderm germ layer (Tam & Loebel, 2007), which then folds and closes to produce the neural tube (Lee et al., 2014). The neural tube folds and bulges to produce vesicles, with the neuroepithelium sheet giving rise to neural stem cells (NSCs) that line the luminal surface of said vesicles (Paridaen & Huttner, 2014). Neuroepithelial (NE) cells thus have apico-basally polarity orientated around the central lumen of the neural tube. Adherens junctions of NSCs segregate the basolateral and apical cell membrane and compartments.

NE cells are early NSCs that expand and generate radial glial cells (RGCs), which through asymmetric division self-renew and produce intermediate progenitor cells and neurons (Gal et al., 2006). Subsequent waves of neuron production lead to inside-out cortical layer formation as deeper layers are formed by earlier-born neurons while more superficial layers are comprised of later-born neurons (Mukhtar & Taylor, 2018).

Within 8 to 12 days of neural induction in in vitro cortical neurogenesis nearly pure cultures of cortical progenitor cells are generated from NSCs, however, the timeline for this crucial step of neuronal differentiation varies amongst cell lines. Generated progenitor cells can be identified by the co-expression of Pax6, Foxg1, Nestin and Vimentin as well as the concurrent decrease in expression of pluripotency markers Oct4 and Nanog (Shi et al., 2012).

Glucose and AMPK signalling

As with all cellular and tissue processes, neurogenesis requires the orchestration of energy status and metabolism. Glucose is a major energy substrate for cells, and through the processes of glycolysis and oxidative phosphorylation, adenosine triphosphate (ATP), the currency of energy, is generated. The adenosine monophosphate-activated protein kinase (AMPK) pathway is an important means by which cells adapt to changes in intracellular ATP levels. A reduction of ATP in relation to adenosine monophosphate (AMP) activates AMPK. This subsequent activation of AMPK leads to the promotion of catabolic reactions but the inhibition of anabolic reactions, thereby restoring ATP levels (Xiao et al., 2011).

AMPK is an obligate heterotrimer which contains a catalytic subunit (α), and two regulatory subunits (β and γ) (Mihaylova & Shaw, 2011). It has been established AMPK can be activated in a two-pronged mechanism. When intracellular levels of ATP are decreased, AMP or adenosine diphosphate (ADP) can bind directly to the γ regulatory subunit. This results in a conformational change which promotes the phosphorylation of AMPK (Xiao et al., 2011). Alternatively, under the conditions of a variety of cellular stress, ADP binds to the γ regulatory subunit leading to AMPK activation (Oakhill et al., 2011). Regardless of mechanism, it is important to note that the phosphorylation of Thr172 in the activation loop, mediated by the serine/threonine kinase LKB1, is essential for AMPK activation (Shaw et al., 2004).

mTOR pathway

AMPK signalling converges onto the central regulator of cell metabolism, the mammalian target of rapamycin (mTOR) pathway which ensures that processes that drive cell growth are balanced against nutrient supply. mTOR is a serine threonine protein kinase that forms the subunits of two protein complexes: mTOR Complex 1 (mTORC1) and 2 (mTORC2) (D.-H.

Kim et al., 2002). mTORC1 is made up of three core components: mTOR, Raptor (regulatory protein associated with mTOR), and mLST8 (mammalian lethal with Sec13 protein 8) (Hara et al., 2002; D.-H. Kim et al., 2002). Raptor is necessary for the proper subcellular localization of mTORC1 and aids substrate recruitment to mTORC1 via binding to the TOR signalling motif found on substrates of mTORC1 (Nojima et al., 2003).

Previous studies have found that hyperglycaemic conditions are associated with mTORC1 hyperactivation (Habib & Liang, 2014; Russo et al., 2012). Conversely, low glucose was reported to increase the AMP:ATP ratio, activating AMPK and subsequently TSC2, which then inhibits mTORC1 (Huynh et al., 2023). In addition to working through TSC2, AMPK can inhibit mTORC1 through the Regulatory-associated protein of mTOR (Raptor) (Gwinn et al., 2008). Another pathway by which low glucose can inhibit mTOR is through stress pathways such as ATF4, which induces GADD34 and thenTSC2, thereby inhibiting mTORC1 (Watanabe et al., 2007).

AMPK activators have proven useful in conditions or events where mTORC1 is hyper-activated. Metformin, the most widely prescribed medication for type 2 diabetes due to its ability to lower blood glucose levels, has proven useful in correcting mTOR hyperactivation in neurodevelopment disorders (Amin et al., 2019). It also inhibits mitochondrial respiratory chain I, leading to a decrease in ATP production and AMPK activation. It is this upregulation of AMPK activity that leads to a decrease in mTOR activation (Hawley et al., 2010).

Tuberous sclerosis complex 2 (TSC2)

Collectively these studies highlight the close relationship between glucose, AMPK, TSC2 and mTORC1. Numerous studies, including in vitro stem cell studies, have also demonstrated

the importance of the mTOR pathway in neurogenesis and this has been most evident in patients with loss of function mutations in TSC2 causing tuberous sclerosis complex (TSC). However, the dynamics and interactions of the mTOR pathway as well as the role of glucose and energy status in the earliest stages of neurogenesis have not been explored previously.

TSC is an autosomal dominant disorder which results from a mutation in either TSC1 (encoding hamartin) or TSC2 (encoding tuberin). TSC is characterized by benign tumours in different organs, with a prominent burden in the central nervous system (Crino et al., 2006). This effect of TSC is theorized to manifest itself through the two-hit hypothesis; the first hit is a congenital lesion of TSC1 or TSC2 and second hit is a loss of heterozygosity of the gene. This lesion reduces the activity of the gene, decreasing its ability to block the phosphorylation of mTOR targets (Inoki et al., 2002; Jozwiak et al., 2008). Neurological impairments arise from a variety of structural abnormalities and tumours including malformed cortical structures known as tubers, and subependymal giant cell astrocytomas. These structural disruptions are associated with various neuropsychiatric manifestations such as epilepsy and autism spectrum disorder, which are collectively known as TSC-associated neuropsychiatric disorders (TAND) (Wong, 2019).

Due to these large variations in disease severity, it becomes challenging to understand the basis of genotype-phenotype correlations in TSC. Previous work has found that TSC2 mutations generate more severe symptoms compared to patients with TSC1 mutations, however, even with the same mutation, there is still great variability in cognitive behavioural deficits (Dabora et al., 2001).

Complete knockout of TSC or TSC1 leads to defective embryogenesis and subsequent lethality meanwhile TSC1 conditional knockout floxed mice causes to apoptotic microcephaly, defected gliogenesis and hamartomas (Carson et al., 2012; Cloëtta et al., 2013; Magri et al., 2011). However, these effects are not as pronounced when compared to the phenotypes of TSC2 knockouts. Additonally, there are significant differences in neuronal development timescales, cell types and migration patterns between rodents and humans (Henske et al., 2016; Soldner & Jaenisch, 2018). With the majority of TSC studies being performed in mouse models, the relevance to human neurodevelopment requires further investigation.

Metabolic pathways during neurogenesis

In the embryonic brain, glucose enters the cells and is first converted to pyruvate via glycolysis. Under aerobic respiration, pyruvate enters the mitochondria and is converted to acetyl-CoA via the pyruvate dehydrogenase complex. This is then converted to citrate via condensation with oxaloacetate in the tricarboxylic acid cycle. The citrate goes through a series of reactions to be decarboxylated back to oxaloacetate which releases carbon dioxide and reducing nicotinamide (NAD) and flavin (FAD) dinucleotides to NADH and $FADH_2$, respectively. The oxidation in the mitochondrial electron transport chain produces an electrochemical gradient in the inner mitochondrial membrane, which drives ATP synthase to form ATP from ADP and molecular phosphate. This is known as oxidative phosphorylation (OXPHOS) (Mitchell, 1961). When oxygen is not available, pyruvate is converted to lactic acid by lactate dehydrogenase (LDH) which results in the production of ATP. This is known as glycolytic metabolism, and whilst not as efficient in producing ATP, cells may rely on glycolysis due to speed of ATP generation (Schurr, 2018).

Astrocytes play a key role in metabolism, converting pyruvate to lactic acid via LDH, which is exported by monocarboxylate transporter (MCT4) to be taken up by neurons. Neurons convert lactate back to pyruvate for later use (Dringen et al., 1993). The main consumers of glucose in the brain are thus astrocytes which have high glycolytic activity (Goyal et al., 2014). Astrocytes act as a defence mechanism for neurons against fluctuations in glucose levels via continuous lactate supply to neurons. It is for this reason mature neurons have low glycolytic activity (Herrero-Mendez et al., 2009), directing pyruvate into oxidative phosphorylation.

In contrast, while NSCs in the subventricular zone have predominantly glycolytic activity, (Kondoh et al., 2007) they are known to be able to switch to OXPHOS (Takubo et al., 2013; J. Zhang et al., 2011). NSCs rely on glycolysis to maintain stemness, and the cellular metabolism in NSCs have been shown to play in integral role in their ability to proliferate or differentiate (Ito & Suda, 2014). During NSC proliferation, increased glycolysis is observed, whereas in NSC differentiation, genes involved in OXPHOS are upregulated (Agostini et al., 2016; Maffezzini et al., 2020). In particular, the switch from glycolysis to OXPHOS is essential for when neurogenesis peaks during mid-embryogenesis or in cortical development when neuronal productions is increased (Mira & Morante, 2020).

When progenitor cells differentiate into neurons, there is reduction in hexokinase 2 and isoform A of LDH which are both glycolytic proteins that metabolise the reduction of pyruvate to lactate (X. Zheng et al., 2016). This shift away from the reduction of pyruvate can also occur through the TP53-inducible glycolysis regulator, TIGAR, which is found to be increased during neuronal development and inhibits glycolysis by regulating hexokinase 2.

TIGAR expression is also associated with increased pyruvate production and decreased lactate levels (Zhou et al., 2019).

In vitro models to recapitulate neurogenesis

To this day, crucial cellular questions about how the most complex organ of the body is derived from a sheet of NEs remain unanswered. Remarkably, this neurogenic programme can be recapitulated in vitro from embryonic and induced pluripotent stem cells. Furthermore, technologies such as CRISPR/cas9 applied to hiPSC or human embryonic stem cells (hESCs) have previously been used to interrogate the role of specific genes in these processes (Hockemeyer & Jaenisch, 2016; Jinek et al., 2013). The development of hiPSCs have made it possible to model cortical brain disorders generating various patient-derived cell lines that can be differentiated into neuronal fates (Vadodaria et al., 2020).

Stem cells can spontaneously, or in a more regulatory fashion with guidance from dual SMAD inhibition, produce NE cells that will self-organise into rosettes that resemble the embryonic neural tube (Zhang et al., 2001). Furthermore, rosette cells have the same properties as radial glia: both are capable of asymmetric division, production of intermediate progenitors and have different layer cortical neurons (Shi et al., 2012). The SMAD signalling pathway is responsible for cell-programmed death, proliferation and inducing neurogenesis. With the use of bone morphogenetic protein (BMP) inhibitors on hESCs, such as SB-431542 and dorsomorphin, neurogenesis is induced in hESCs and the cells are prevented from acquiring a trophoblastic characteristic or pluripotency (Chambers et al., 2009). Fibroblast growth factor-2 (FGF2) can also be used to stimulate efficient NSC proliferation. Once NSCs differentiate into progenitor cells, FGF2 is used to maintain progenitor cell populations and prevents further differentiation (Woodbury & Ikezu, 2014).

In vitro culture conditions for a majority of patient derived NSC studies do not necessarily mimic physiological conditions as they tend to use glucose concentrations of 25 mM. For comparison, in euglycemic adult brains glucose concentrations tend to range between 1-2.5 mM depending on neuronal activity levels (Ritter, 2017). Similarly, the threshold for neonatal hypoglycaemia is 2.2mM but, in neonatal studies investigating effects of glycaemia in preterm infants hyperglycaemia has been defined as glucose concentrations above 8.3 mM (Naseh et al., 2022; Stanescu & Stoicescu, 2014).

The overall goal of this study was to better understand how glucose supply affected energy status and mTOR pathway activity by using embryonic stem cells differentiated into neuroepithelium to model early neurogenesis.

Specific Aims

The specific aims of this study were as follows:

1) Determine ATP levels and AMPK activity during the period of neuroepithelial sheet formation, under hyperglycaemic and physiological glucose conditions.

2) Determine the relationship between glucose supply and mTORC1 activity and whether metformin can reverse effects of elevated glucose.

3) Investigate whether TSC2 is necessary for effects of elevated glucose and metformin on mTORC1 activity.

The hypothesis for this study is that at different time-points of differentiation into the neuroepithelial sheet, energy status and corresponding activities of AMPK and mTORC1 change to balance nutrient supply (glucose) with metabolic activity. Furthermore, based on previous literature, increased glucose supply is expected to reduce the AMPK:ATP ratio to

then inhibit AMPK and activate mTORC1 through TSC2 inhibition. Metformin, an AMPK activator, is expected to reverse these effects. Finally, without TSC2, changes in glucose and metformin should minimally affect mTORC1 activity

Methods

Human embryonic stem cell lines

Human embryonic stem cells (hESCs) were obtained from La Hoffmann-Roche Limited whereas hES harbouring a TSC2 deletion (TSC2-/-) were created by neomycin selection cassette into both TSC2 alleles. The isogenic control line (TSC2+/+) was created by insertion into the AAVS1 safe harbour locus of the well-characterized hES line SA001 (Costa et al., 2016; Rocktäschel et al., 2019).

Human embryonic stem cell line maintenance and passaging

The hESCs were grown on Matrigel-coated cell culture plates (Corning) in mTeSR™1 (STEMCell Technologies) at 37°C with a 5% CO_2 concentration. Media was changed daily with regular passaging with Ethylenediaminetetraacetic acid (EDTA) (Invitrogen) when confluency reached 80 to 90%. For passaging, cells were washed with Dulbecco's phosphate-buffered saline (DPBS) (Gibco) then 0.5 mM of pre-warmed EDTA. 0.5 mM EDTA was then added to wells and cells were incubated for 2 minutes at 37°C with a 5% CO_2 concentration. EDTA was then removed and gently flushed with mTeSR™1 without breaking colonies into single-cell and transferred to Matrigel-coated 6-well plates.

Neuronal differentiation from TSC2 +/+ and TSC2 -/-

hESCs were differentiated using a well-established dual SMAD inhibition protocol into neuroepithelial sheets as first described by Shi et al. (2012). At 100% confluency, hESCs

were induced with neural induction media (NIM) and kept in NIM with daily media changes for 12 days. NIM involves neural maintenance media (NMM) supplemented with 1 μM dorsomorphin (Tocris Bioscience) and 10 μM SB431542 (Tocris Bioscience).
High glucose NMM [25mM] was made with a 1:1 mixture of DMEM w/o glucose (Gibco) and Neuronal basal medium w/o glucose (Gibco) supplemented with 1% B27 w/o vitamin A (Gibco), 0.5% N2 (Gibco), 50 μM beta-mercaptoethanol (Gibco), 1mM glutaMAX-I (Gibco), 25 U/ml Penicillin-streptomycin (Gibco), 2.5 μg/ml insulin (Sigma-Aldrich), 0.5mM sodium pyruvate (Sigma- Aldrich), 50 μM minimal essential medium with NEAA w/o glutamine (Gibco), and 25 mM D-glucose (Gibco). Physiological glucose NMM [5mM] was made with the same concentration of media and supplements above but with 5 mM D-glucose (Gibco) **(Table 1)**.

Metformin treatment

Metformin (Tocris Bioscience) was prepared in distilled water used at a final concentration of 1 μM. At days 0, 5 and 11, cells were treated with Metformin [1 μM] for 24 hours.

Immunocytochemistry

Cells were washed with DPBS and fixed with 4% paraformaldehyde (PFA) (Agar Scientific) for 10 minutes. The cells were then washed with DPBS two times and stored at 4°C until staining. Cells were permeabilized with 0.1% Triton X-100 (Sigma-Aldrich) in DPBS for 15 minutes before being blocked with 10% goat serum (Sigma-Aldrich) for an hour. Cells were then incubated overnight (at least 16 hours) at 4°C with 1:500 of primary antibody in 5% goat serum. The following day, cells were washed twice with DPBS for five minutes each time. The cultures were then incubated with secondary antibody at 1:1000 in 5% goat serum in dark for one hour. The cultures were then washed three times with DPBS for five minutes

before being incubated in the dark for 10 minutes at room temperature in 1X 4',6-Diamidino-2-Phenylindole (DAPI) (Sigma-Aldrich). The following antibodies were used: anti-PAX6 (rabbit, Abcam ab5790), anti-Nestin (mouse, Abcam ab22035), anti-rabbit IgG Alexa Fluor 594 (goat, Invitrogen A-11037), anti-mouse IgG, Alexa Fluor 488 (goat, Invitrogen A-11029). Imaging was performed using the EVOS M7000 Imaging System (Thermo Fisher) and processed using ImageJ/FIJI.

RNA Extraction

RNA was extracted using the Direct-zol™ RNA Microprep kit (ZYMO RESEARCH). Cell pellets were lysed in 150 µL of TRIzol reagent and mixed with an equal amount of 100% ethanol. Supernatant was collected and loaded into an RNA extraction column and centrifuged at 150g for 30 seconds. The RNA extraction column was then placed on a new extraction tube to remove TRIzol trace. 400 µL of Direct-zol™ RNA prewash was added to the column and centrifuged at 150g for 30 seconds, with this step being repeated once. The column then had 700 µL of RNA wash buffer added and centrifuged at 150g for 60 seconds. Lastly, the RNA collection column was eluted using 15 µL DNase/Rnase-Free water through centrifugation at 150g for 30 seconds. Nanodrop 2000/2000c spectrophotometer (Thermo Fisher) was used to measure quality and concentration of isolated RNA.

Determination of gene expression

Conversion of 150 ng RNA to cDNA using reverse transcription was performed using the SuperScript IV First-Strand Synthesis System (Invitrogen) kit. Firstly, a reaction mixture was prepared to be 13 µL from 1µl of 50 ng/µl random hexamers, 1µl of 10 mM dNTP, 150 ng of the extracted RNA template and DEPC-treated water (Invitrogen). This was incubated at 65°C for five minutes followed by incubation on ice for at least one minute. Then, 4µl of

SSIV buffer, 1 µL of 100mM DTT, 1 µL of Ribonuclease inhibitor and 1 µL of Superscript IV Reverse Transcriptase were added and mixed with the previous reaction mixture. This was then incubated at 23°C for 10 minutes, then 55°C for 10 minutes and finally 80°C for 10 minutes for cDNA synthesis. cDNA samples were used for Quantitative real-time PCR (qRT-PCR) or stored at -20°C.

StepOnePlus real-time PCR system (Applied Biosystems) with SYBR green was used to perform qRT-PCR. Reaction was prepared with 0.9µL of forward primer **(Table 2)**, 0.9µl of reverse primer **(Table 2)**, 2µl of cDNA, 10µl SYBR™ Green PCR Master Mix (Applied Biosystems) and 6.2µl nuclease-free water. Primers were retrieved from PrimerBLAST. GAPDH and b-Actin were used as the housekeeping gene for which data was normalized. There was no significant difference in expression of housekeeping genes GAPDH and bActin between hyperglycaemic and normoglycemic conditions, in both TSC2 +/+ and TSC2 -/-. The $2^{-\Delta CT}$ was used to calculate mRNA abundance.

ATP assay

hESCs were split into single cell using accutase (STEMCell Technologies) and seeded in sterile white 96-well plates (Thermo Fisher) at 0.02×10^6 cells/well where they were grown in 100 µL media/well. To measure ATP levels, the Luminescent ATP Detection Assay Kit (Abcam) was used. ATP levels were measured through light production from the reaction of ATP and firefly's luciferase and luciferin. On empty wells of 96-well plate, ATP standards were prepared at 1 µM, 0.1 µM, 0.01 µM, 0.001 µM, 0.0001 µM, 0.00001 µM in NMM. All cultured wells had fresh NMM before 50 µL of detergent was added. The plate was sealed and placed on orbital shaker for five minutes at 650 rpm to lyse cells and stabilize ATP. 50 µL of substrate solution was added to each well before being plate was sealed and placed on

orbital shaker for five minutes at 650 rpm. The plate was then placed in the dark at room temperature for ten minutes. Luminescence was then measured.

Western Blotting

Protein extraction: Cell pellets were collected and mixed with 1X lysis buffer phosphatase–proteinase inhibitor (Thermo Scientific) in Radioimmunoprecipitation assay buffer (RIPA) (Thermo Scientific). Cells were incubated in the lysis buffer for thirty minutes on ice and vortexed every five minutes. Samples were centrifuged at 14000 rpm for five minutes at 4°C. The supernatant was then collected for protein estimation using Pierce BCA Protein Assay (Thermo Fisher).

Protein estimation: 10 µL of standard or unknown sample was placed into a microplate well in a 96-well plate. 80 µL of working reagent was then added to each well before being placed on orbital shaker for 30 seconds at 650 rpm (Pierce™ BCA Protein Assay Kit, 23227). The plate was then covered and incubated at 37°C for 30 minutes. The plate was then cooled to room temperature and had absorbance measured at 562 nm on plate reader. Using BSA standard, 10 µg of protein was calculated for western blotting.

10 µg of sample in 10 µl mix of sample, NuPAGE™ LDS Sample Buffer (4X), NuPAGE™ Reducing Agent (10X) and Deionized Water were run on NuPAGE™ 4–12% Bis-Tris gels (Invitrogen) for 45 minutes at 200 volts in MOPS SDS Running Buffer (life technologies). The gel was then transferred to a nitrocellulose membrane using the Bio-Rad Trans-Blot Turbo Transfer System.

The iBind Flex Western Device (Thermo Fisher) was used to block and incubate antibodies using sequential lateral flow. Membranes were placed in system for 16 hours. The housekeeping antibody was anti-bActin (mouse, Abcam ab8227, 1:2000). The following antibodies were used: anti-pS6 (rabbit, Cell Signalling 4858s, 1:1000), anti-S6 (rabbit, Cell

Signalling 4856, 1:1000), anti-pAMPK (rabbit, Cell Signalling 2535, 1:1000), anti-AMPK (rabbit, Cell Signalling 5832, 1:1000). Protein quantifications were normalized to bActin for pAMPK/AMPK **(Appendix: Figure 9)** and pS6/S6 **(Appendix: Figure 10)** ratios were calculated from blots imaged by Odyssey DLx Imager (LI-COR Bioscience) **(Appendix: Figure 11, 12)**.

Statistical Analysis

GraphPad Prism Version 10 was used to plot figures from 3 biological replicates. Data was analyzed using a two-way analysis of variance (ANOVA). with post-hoc Šídák test where appropriate, with $p<0.05$ considered as significant ($p\geq 0.05$ (ns), <0.05 (*), <0.01 (**), <0.001 (***), <0.0001 (****)).

Results

Confirmation of neuroepithelial sheet formation

Immunofluorescence microscopy and qRT-PCR of TSC2 +/+ and TSC2 -/- cell lines showed hESC characteristics at day 1 (24 hours after induction of neurulation) with progression towards a neuroepithelial state by day 12 **(Figure 1)**. Already by day 1, expression of pluripotency genes SOX2 and Nanog were at low levels, whilst OCT4 substantially reduced by Day 6 **(Figure 1C)**. This was true in normoglycaemic and hyperglycaemic conditions and irrespective of cell genotype.

Between day 1 and 12 in TSC2 +/+, there was an increase in Pax6, the transcription regulatory that controls expression of neuronal genes and determination of neural progenitor cells in both hyperglycaemic and normoglycaemic conditions as observed in multiple fields of view in ICC (X. Zhang et al., 2010) **(Figure 1A)**. This same increase in Pax6 expression across both conditions was also observed in TSC2 -/- cells **(Figure 1B).** Between day 1 and 12 in TSC2 +/+ and TSC2 -/- cell lines, mRNA abundance of Pax6 had a significant increase, two-way ANOVA ($F_{3,24}$= 26.96, $p<0.0001$). The increase in Pax6 was accompanied by a visible increase in Nestin across multiple fields of view in ICC between day 1 and 12 in TSC2 +/+ and TSC2 -/- cell lines in both hyperglycaemic and normoglycemic conditions **(Figure 1A, B)**. Nestin is an intermediate filament protein which maintain the structural integrity of neural stem and progenitor cells and is found in sites of active neurogenesis (Suzuki et al., 2010). Gene expression of Nestin also increased between day 1 and 12 in TSC2 +/+ and TSC2 -/- cell lines across all conditions ($F_{3,24}$=166.2, $p<0.0001$). Under normoglycaemic conditions, TSC2 -/- already showed rosette-like formations, perhaps suggesting an accelerated neurogenesis **(Figure 1B)**.

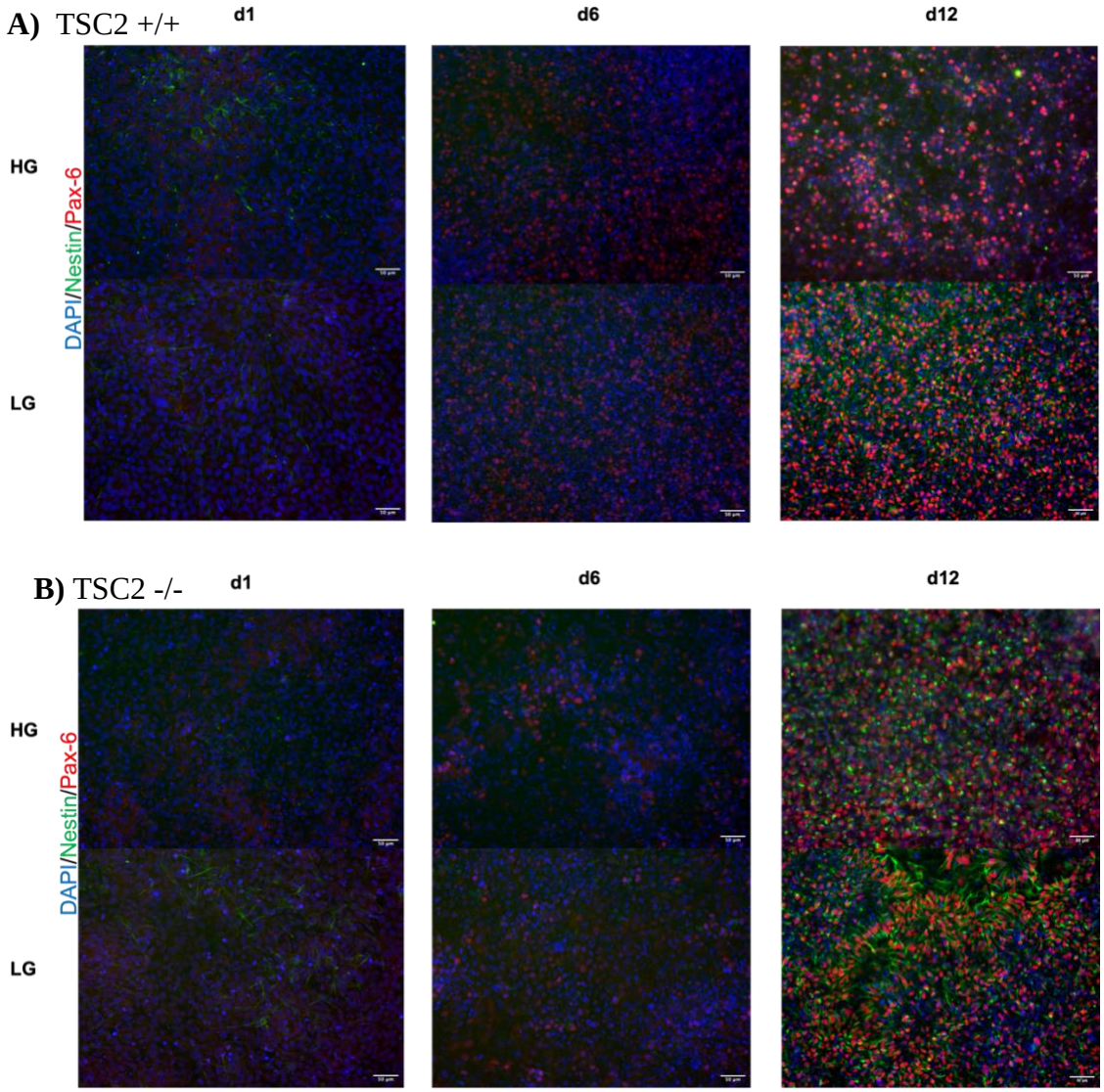
A) TSC2 +/+
d1
d6
d12
HG
LG
DAPI/Nestin/Pax-6
B) TSC2 -/-
d1
d6
d12
HG
LG
DAPI/Nestin/Pax-6

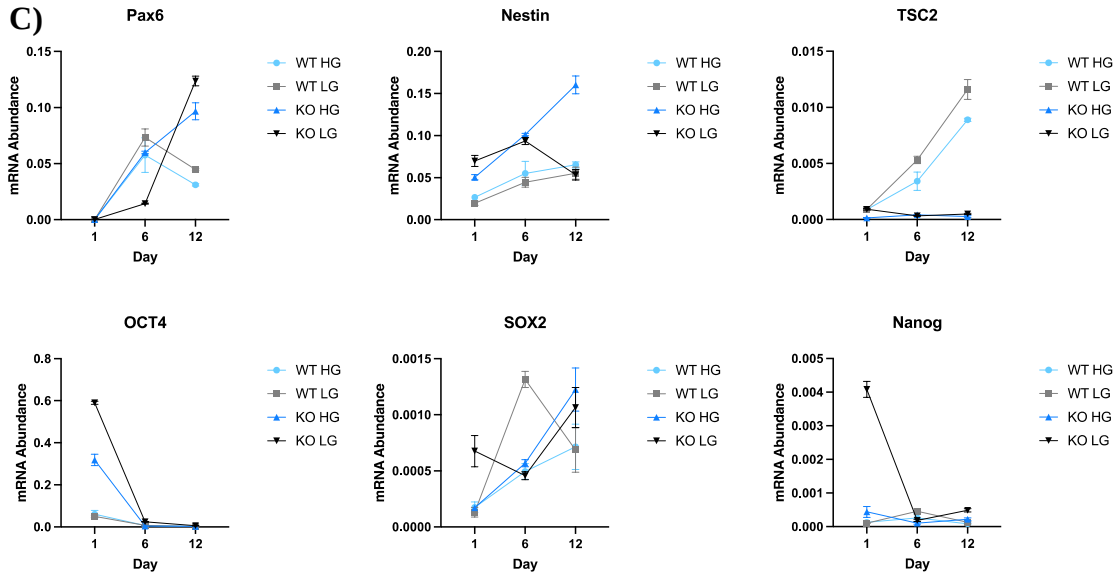
C)
Pax6
Nestin
TSC2
OCT4
SOX2
Nanog
mRNA Abundance
Day
WT HG
WT LG
KO HG
KO LG

Figure 1: Successful formation of neuroepithelial sheet from isogenic control and TSC2 knockout generated from hESCs. Immunofluorescence confirming the expression of Nestin (neural progenitor marker, green), Pax6 (early neuroepithelial marker, red) and DAPI (nucleus marker, blue); scale bar 50 µm. A) Immunofluorescence of TSC2 +/+ confirmed expression of Nestin and Pax6 in both high glucose (HG) [25mM] and low glucose (LG) [5mM] media. B) Immunofluorescence of TSC2 -/- confirmed expression of Nestin and Pax6 in both high glucose (HG) [25mM] and low glucose (LG) [5mM] media. C) qRT-PCR at Days 1, 6 and 12 confirmed a significant increase in Pax6 over differentiation time in both TSC2 +/+ (WT) and TSC2 -/- (KO) under hyperglycaemic and normoglycaemic conditions. Nestin had a significant increase over 12-day induction in all cells under both conditions except for TSC2 -/- in LG. TSC2 significantly increased in WT cells over differentiation time and confirmed KO cell line. Pluripotency marker Oc4 significantly decreased over differentiation time in all cell lines under both conditions. Pluripotency markers Sox2 and Nanog after one day of induction were at insignificant levels. The significance was calculated using data from three biological replicates $p \geq 0.05$ (ns), <0.05 (*), <0.01 (**), <0.001 (***), <0.0001 (****).

Energy status is stable in early neurogenesis in wildtype cells irrespective of glucose supply

ATP levels increased as neurogenesis progressed; two-way ANOVA ($F_{2,12}=17.83$, $p=0.0003$) **(Figure 2A)**. However, cells did not show any difference in ATP levels at any time-point between hyperglycaemia and normoglycaemia; two-way ANOVA ($F_{1,12}=0.1031$, $p=0.7536$). AMPK activation is an important energy sensor inversely correlated with ATP levels. Whilst not significant, AMPK activation was lowest at Day 12, coinciding with the peak of ATP levels. AMPK activity had non-significantly decreased overtime in hyperglycaemic conditions.

Furthermore, as expected from the lack of difference in ATP levels, there was no difference between hyperglycaemic and normoglycaemic conditions **(Figure 2B)**.

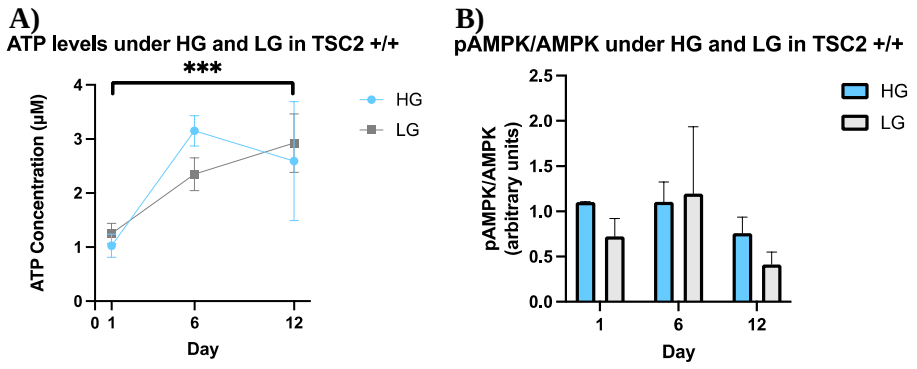

Figure 2: The effect of hyperglycaemic and normoglycaemic conditions on ATP levels and AMPK activity in isogenic control cells as they differentiate to neuroepithelium. A) ATP levels increased over differentiation time in both high glucose (HG) [25mM] and low glucose (LG) [5mM] between Day 1 and 12. B) AMPK activity was stable in isogenic control (TSC2 +/+) across all time-points between HG and LG conditions. The significance was calculated using data from three biological replicates $p \geq 0.05$ (ns), <0.05 (*), <0.01 (**), <0.001 (***), <0.0001 (****).

Hyperglycaemia alters mTORC1 dynamics associated with differentiation to neuroepithelium

mTOR activation peaked at Day 1 in normoglycaemia and substantially reduced thereafter. In hyperglycaemia, the mTORC1 peak shifted to Day 6. This meant there were significant differences at Day 1 and Day 6 depending on glucose supply – with a significant reduction of mTOR activation in hyperglycaemia relative to normoglycameia at Day 1 (95%CI: -0.8511, -0.4383; $p<0.0001$) and a significant increase at Day 6 (95%CI: 2.070, 2.483; $p<0.0001$). At day 12, there was no significant difference in mTORC1 activity between hyperglycaemic and

normoglycaemic conditions (95%CI: -0.05760, 0.3552; p=0.7367) **(Figure 3)**. This data also indicates that in normal neurogenesis mTOR activity is downregulated at an early stage.

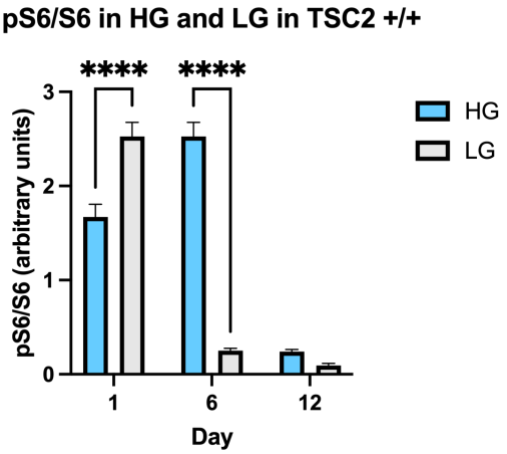

Figure 3: The effect of hyperglycaemic and normoglycaemic conditions on mTORC1 activity in isogenic control as they differentiate to neuroepithelium. mTORC1 activity peaked at Day 6 in isogenic control cells (TSC2+/+) and reduced significantly by Day 12 under high glucose (HG) [25mM] condition. In low glucose (LG) [5mM], mTORC1 started elevated at Day 1 and decreased over 12-day differentiation. The significance was calculated using data from three biological replicates p≥ 0.05 (ns), <0.05 (*), <0.01 (**), <0.001 (***), <0.0001 (****).

Metformin effects are dependent on glucose supply and differentiation time-point

Metformin is an established AMPK activator (Amin et al., 2019). When wildtype cells were treated with metformin, AMPK activity gradually decreased over time under normoglycaemic conditions **(Figure 4A)**. In contrast, metformin significantly increased AMPK activation in hyperglycaemic conditions only at day 12 (95%CI: -0.9441, -0.1806; p=0.0059) and a significant decrease in AMPK activation at day 6 (95%CI: 0.0007492, 0.6836; p=0.0495) **(Figure 4B)**.

Metformin did not affect ATP levels in either normoglycemic or hyperglycaemic conditions. In hyperglycaemic conditions, ATP levels peaked at day 6 with and without metformin treatment **(Figure 4C)**. In normoglycaemic conditions, ATP levels peaked at day 12 with and without metformin treatment **(Figure 4D)**.

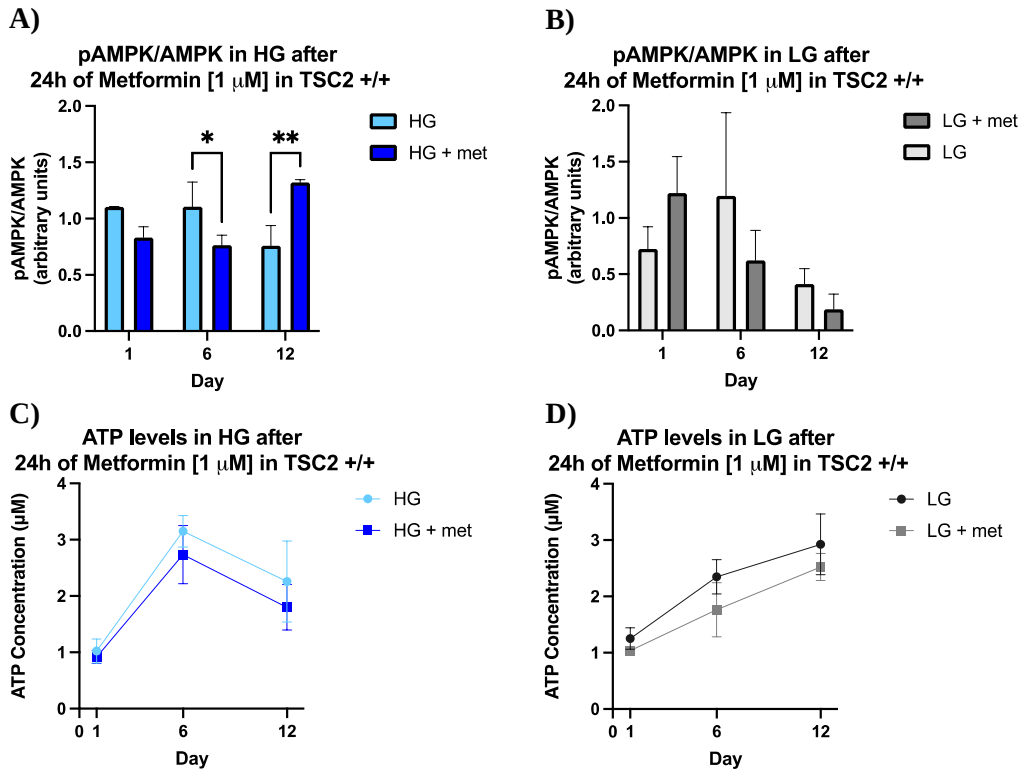

Figure 4: The effect of hyperglycaemic and normoglycaemic conditions on ATP levels and AMPK activity in isogenic control. A) After 24 hours of Metformin treatment [1μM] AMPK activity decreased at Day 6 whilst increasing activity at Day 12 in isogenic control cells (TSC2+/+) under high glucose (HG) [25mM] condition. B) Metformin had no effect on AMPK activity in TSC2+/+ cells at any time-point under low glucose (LG) [5mM] condition. With metformin, AMPK activity in LG was elevated at Day 1 and decreased over differentiation time. C) Metformin had no effect on ATP levels under HG where levels peaked at Day 6. D) Metformin had no differential effect on ATP levels under LG in which under both conditions ATP levels increased between Day 1 and Day 12. The significance was calculated using data

from three biological replicates p≥ 0.05 (ns), <0.05 (*), <0.01 (**), <0.001 (***), <0.0001 (****).

Loss of TSC2 results in dysregulated energy status during early neurogenesis

Overall ATP levels were lower in TSC2 -/- compared to isogenic wildtype cells **(Figure 5B)**. As with wildtype cells, there was an increase in ATP with differentiation time. However, TSC2 -/- cells in hyperglycaemic conditions compared to normoglycaemia had greater ATP levels particularly at Day 6 (95%CI: 0.3314, 0.7601; p=0.0005) but also Day 12 (95%CI: 0.03005, 0.4587; p=0.0288) **(Figure 5A)**.

AMPK activation dynamics in TSC2-/- in normoglycaemic conditions are very different to wildtype cells, with a substantial elevation at Day 12. This dynamic is different again in TSC2-/- cells in hyperglycaemic conditions with AMPK activity peaking at Day 1 and then decreasing. This leads to a large difference when comparing AMPK activation at Day 12 between high and low glucose (95%CI: -7.699, -4.740; p<0.0001). There was no significant difference in AMPK activity amongst conditions at Day 1 and 6 **(Figure 5C)**. When compared to wildtype cells, AMPK activity appeared to be similar only at day 6 across all conditions **(Figure D)**.

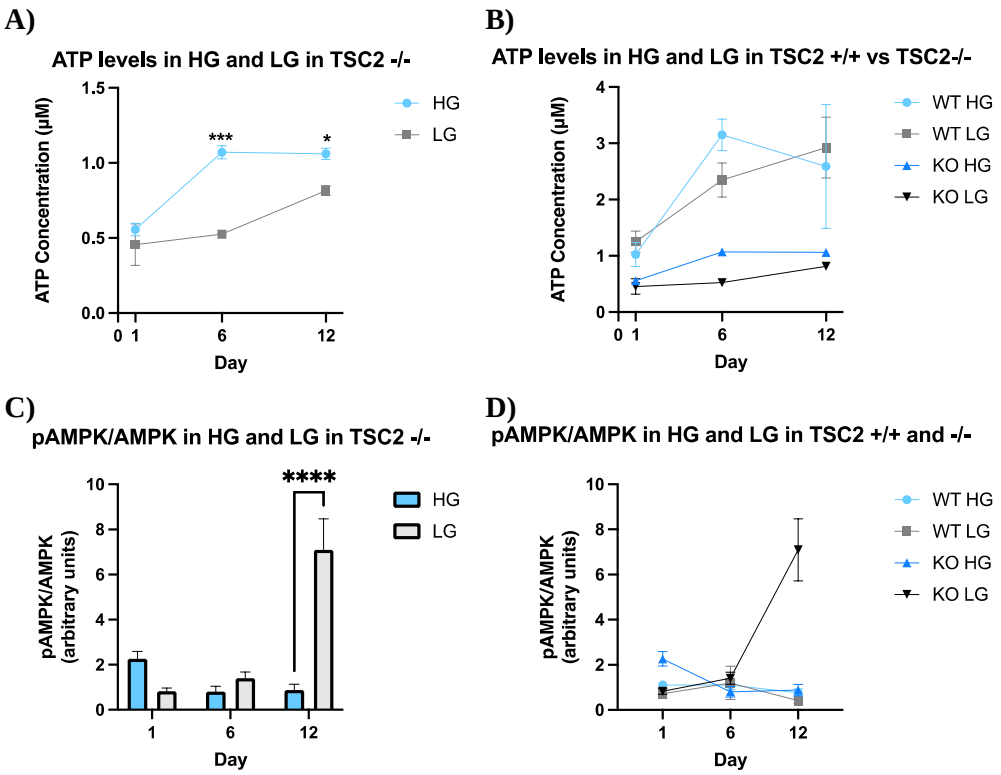

Figure 5: Effect of hyperglycaemic and normoglycaemic conditions on ATP levels and AMPK activity in TSC2-/- cells. A) ATP levels increased in both high glucose (HG) [25mM] and low glucose (LG) [5mM] conditions between Day 1 and Day 12. ATP levels in HG were significantly increased at Day 6 and Day 12 compared to cells in LG. B) Overall ATP levels were increased in isogenic control compared to TSC2 -/- cells. C) AMPK activity slowly decreased over differentiation time in HG whereas activity increased between Day 1 and Day 12 in LG. D) Overall AMPK activity was similar at Day 6 with both cell types under HG and LG having decreased levels with the exception of a large elevation in AMPK activity in TSC2 -/- cells in LG. The significance was calculated using data from three biological replicates $p \geq 0.05$ (ns), <0.05 (*), <0.01 (**), <0.001 (***), <0.0001 (****).

24-hour metformin treatment reduced the hyper-activated AMPK at Day 12 in TSC2 -/- cells in normoglycaemic conditions (95%CI: 4.353, 7.808; $p<0.0001$) **(Figure 6B)** and at Day 1 in TSC2 -/- cells in hyperglycaemic conditions (95%CI: 0.5333, 1.793; $p=0.0013$) **(Figure 6A)**.

Metformin had no substantial effects on ATP levels in TSC2 -/- cells except at Day 12 in hyperglycaemic conditions where it appeared to restore ATP to levels seen in wildtype cells (95%CI: -1.513, -0.7159; p=0.0003) **(Figure 6C)**. Under normoglycaemic conditions, metformin only had an effect on ATP levels at Day 12 where it had a significant increase (95%CI: -0.5939, -0.1087; p=0.0095) **(Figure 6D)**.

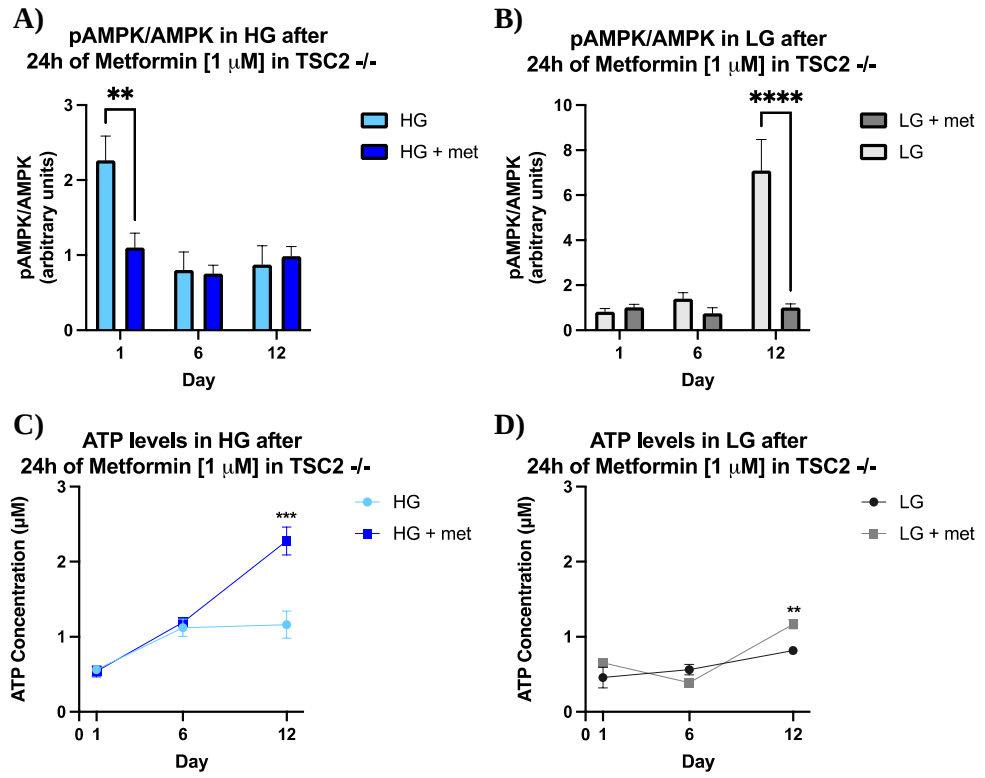

Figure 6: Effect of Metformin in hyperglycaemic and normoglycaemic conditions on ATP levels and AMPK activity in TSC2-/-. A) 24-hour Metformin treatment [1μM] decreased AMPK activity in TSC -/- cells under high glucose (HG) [25mM] condition at Day 1 and had no effect at Day 6 or Day 12. B) Metformin decreased AMPK activity in TSC -/- cells under low glucose (LG) [5mM] condition at Day 12 and had no effect at Day 1 or Day 6. C) Metformin increased ATP levels at Day 12 in TSC -/- cells under HG. D) Metformin only increased ATP levels at Day 12 in TSC -/- cells under LG. The significance was calculated

using data from three biological replicates p≥ 0.05 (ns), <0.05 (*), <0.01 (**), <0.001 (***), <0.0001 (****).

Glucose supply but not metformin affects mTOR activity in the absence of TSC2 during early neurogenesis

Under normogylcaemic conditions, TSC2-/- cells compared to isogenic wildtype cells showed the expected elevated mTORC1 activity at Day 6 and Day 12 **(Figure 7C)**. In TSC2 -/- cells, hyperglycaemic conditions were associated with a significant reduction in mTORC1 activation; two-way ANOVA ($F_{1,12}$=167.2, p<0.0001) **(Figure 7A)**. The increase in mTORC1 activity gradually increased over differentiation time between day 1 (95%CI: -1.263, -0.4166; p=0.0008) and Day 12 (95%CI: -1.725, -0.8788; p<0.0001) in normoglycaemic conditions when compared to TSC2 -/- cells under hyperglycaemic conditions **(Figure 7C)**. Under hyperglycaemic conditions, mTORC1 activity was significantly increased in wildtype cells when compared to TSC2 -/- cells at Day 1 (95%CI: 1.168, 1.702; p<0.0001) **(Figure 7B)**. This trend remained significantly increased at Day 6, however, at Day 12, TSC2 -/- cells had a significant increase in mTORC1 activity when compared to wildtype cells in hyperglycaemic conditions (95%CI: -0.8721, -0.2758; p=0.0006) **(Figure 7B)**. This trend in mTORC1 activity occurred faster in normoglycaemic conditions. Under normoglycaemic conditions, mTORC1 activity was significantly increased in wildtype cells when compared to TSC2 -/- cells at Day 1 (95%CI: 1.074, 1.827; p<0.0001) **(Figure 7C)**. TSC2 -/- cells under normoglycaemic conditions had a significant increase in mTORC1 activity at Day 6 (95%CI: -1.676, -0.9233; p<0.0001) and 12 (95%CI: -2.361, -1.688; p<0.0001) **(Figure 7C)**.

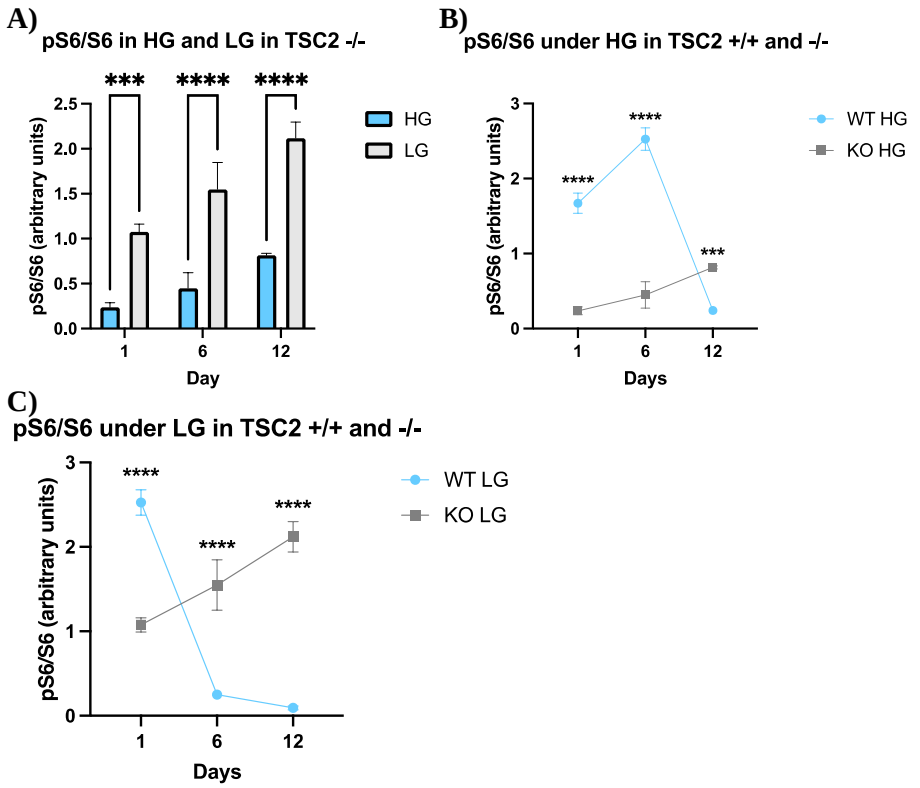

Figure 7: Effect of hyperglycaemic and normoglycaemic conditions on mTORC1 activity in isogenic control and TSC2 -/-. A) mTORC1 activity was increased in TSC2 -/- cells under low glucose (LG) [5mM] conditions when compared to high glucose (HG) [25mM] conditions across all time-points. B) Isogenic control (TSC2 +/+) cells under HG presented with an increase in mTORC1 activity at Day 1 and Day 6 when compared to TSC2 -/- cells. This trend was reversed at Day 12. C) in LG conditions, TSC2 +/+ cells had increased mTORC1 activity compared to TSC2 -/- cells at Day 1 but were decreased at Day 6 and Day 12. The significance was calculated using data from three biological replicates $p \geq 0.05$ (ns), <0.05 (*), <0.01 (**), <0.001 (***), <0.0001 (****).

Lastly, metformin, despite being able to normalise AMPK activation at day 12, had no substantial effect on mTOR activation in TSC2 -/- cells in either hyperglycaemic ($F_{1,10}$=1.1314, p>0.05) **(Figure 8A)** or normoglycaemic conditions ($F_{1,10}$=0.03539, p>0.05) **(Figure 8B)** at any time-point, as determined by a two-way ANOVA.

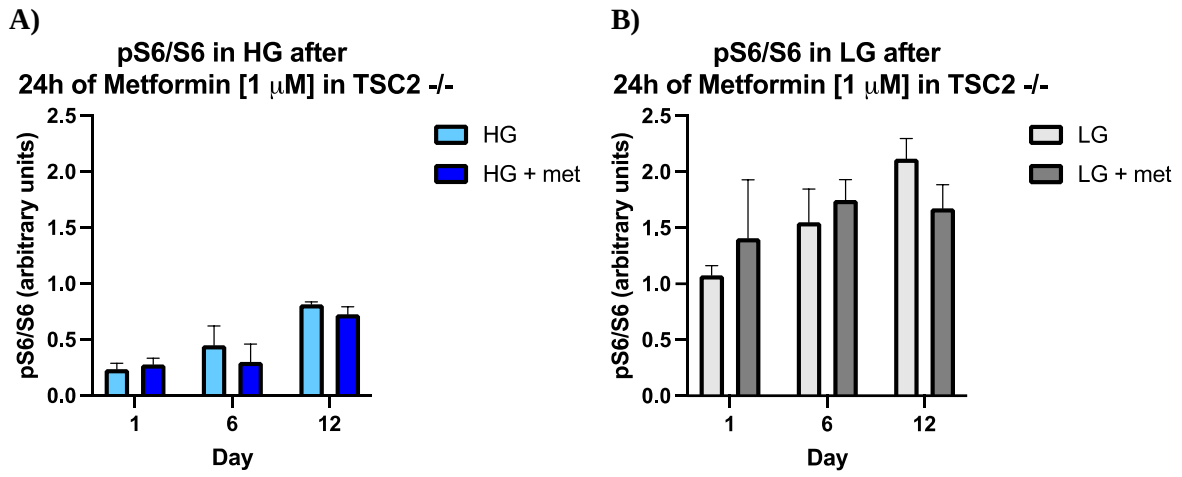

Figure 8: Effect of Metformin in hyperglycaemic and normoglycaemic conditions on mTOR activity in TSC2-/-. A) 24-hour Metformin treatment [1μM] had no effect on mTORC1 activity under high glucose (HG) [25mM]. B) Metformin treatment had no effect on mTORC1 activity under low glucose (LG) [5mM]. The significance was calculated using data from three biological replicates p≥ 0.05 (ns), <0.05 (*), <0.01 (**), <0.001 (***), <0.0001 (****).

Discussion

This study has uncovered complex and changing relationships between glucose supply, ATP, AMPK and mTORC1. ATP levels increase with differentiation time, which may reflect upregulation of catabolic pathways to support growing energy needs during neurogenesis and is consistent with findings from other studies (Agostini et al., 2016; Maffezzini et al., 2020; X. Zheng et al., 2016). AMPK activation was stable, and this may suggest that AMP levels are also rising in parallel with ATP since it is the change in ratio of AMP:ATP which activates AMPK. Hence, contrary to the starting hypothesis, altering glucose supply did not affect ATP

levels or AMPK activation. This may suggest that early in neurogenesis, other necessary factors for induced AMPK activation are not present.

Loss of TSC2 appears to result in dysregulation in energy status in early neurogenesis with reduced ATP levels in TSC2 -/- compared to isogenic wildtype cells. Hyperglycaemic conditions slightly increased ATP but did not restore this to levels seen in wildtype cells. This is aligned with a study that found TSC2-deficieint neurons generated from homozygous TSC2 mutant iPSC lines have impaired mitochondrial bioenergetics with decreased ATP turnover (Ebrahimi-Fakhari et al., 2016). As with wildtype cells, AMPK activity did not significantly change in relation to ATP levels. However, in one specific condition – Day 12, normogylcaemia, TSC2 -/- cells show a dramatically elevated AMPK activation. A previous study has shown inactivation of TSC2 in mouse embryonic fibroblasts activates AMPK activity, but this was thought to arise from an altered AMP/ATP ratio (Hahn-Windgassen et al., 2005). Another study found that when AMPK activity is increased, glucose uptake is stimulated, by increasing GLUT4, in order to provide the substrates for energy production (Richter & Ruderman, 2009). In order to understand why AMPK is not activated as expected when ATP is low and then hyper-activated at Day 12 in TSC2 -/-, it will be important in future studies to measure AMP levels and whether changes in GLUT4 or glucose uptake may contribute to dysfunctional energy states.

Although glycolysis produces less ATP than OXPHOS, its kinetics are faster and could support the proliferation in NE sheet formation at this early time-point (Lunt & Vander Heiden, 2011). However NSCs differentiating into neurons downregulate glycolysis (Shin et al., 2015) and upregulate OXPHOS-specific genes (Maffezzini et al., 2020). As NSCs differentiate into RGCs and progenitor cells, the mitochondria transitions from a fragmented to elongated state which

alters its activity (Maffezzini et al., 2020). This is partly due to the regulation of mitochondria cristae where effectors of OXPHOS and the electron transport chain is located (Pernas & Scorrano, 2016). Mitochondrial fusion also appears important for radial glial cell renewal and agents which disrupt mitochondrial fusion genes such as mitofusin 1 and 2 (MFN1/2) leading to increased neuronal differentiation due to a decrease in RGC self-renewal. Cells in high glucose display increased fragmentation and decreased MFN1/2 (Y. Zheng et al., 2021). In this context, it would be interesting to investigate in future studies, changes in mitochondrial morphology in TSC2 -/- cells and whether this may contribute to the lower levels of ATP.

The dynamics of mTORC1 in wildtype cells is interesting, which was measured on Day 1 (24 hours after starting differentiation), Day 6 and Day 12. mTORC1 activity peaked at Day 6 under hyperglycaemic conditions whereas under normoglycemic conditions, mTORC1 activity was already at its highest on Day 1. Previous studies have indicated that mTORC1 activity is kept at low levels to maintain stemness (Easley et al., 2010; LiCausi & Hartman, 2018). There is reduced translation of p70 S6K, which encodes for S6 Kinase (S6K, which phosphorylates the S6 ribosomal protein) to maintain an undifferentiated state (Easley et al., 2010). Conversely, elevations in mTORC1 signalling can lead to a loss of stemness (Easley et al., 2010). Furthermore, it has previously been shown that mTORC1 activation enables generation of Tbr2+ intermediate progenitor cells (Díaz-Alonso et al., 2015). My data suggests an early sharp increase in mTORC1 activity as differentiation commences followed by rapid downregulation as the neuro-epithelial sheet is formed. In hyperglycaemic conditions, the elevation in mTORC1 activity persists until at least Day 6.

TSC2 is an important negative regulator of mTORC1 with loss of TSC2 expected to lead to over-activation of mTORC1. The loss of one or both alleles causes mTORC1 activation in

patient-derived iPSC neurons. Surprisingly then mTORC1 activity was greater in wildtype cells than TSC2 -/- cells at Day 1 in normoglycaemic conditions and Day 1 and 6 in hyperglycaemic conditions. Furthermore, in TSC2 -/- cells, hyperglycaemia consistently downregulated mTORC1 activity. This suggests that in the very earliest stages of neurogenesis, regulators other than TSC2 dominate to determine mTORC1 activity. It also suggests that in TSC2 -/- cells, additional mechanisms to supress mTORC1 activity are recruited, which then prevents the brief upregulation of mTORC1 evident in wild type cells in early neurulation. An interesting candidate in this respect is DEP domain-containing mTOR interacting protein (DEPTOR) - an endogenous mTOR inhibitor upregulated in undifferentiated stem cells and immediately downregulated when differentiation commences (Agrawal et al., 2014).

Reactive oxygen species (ROS), is another plausible mechanism. A previous study has reported that high glucose supply through cellular stress can lead to inhibition of mTORC1 (Sarbassov et al., 2005), perhaps through generation of ROS which can be produced under conditions of hyperglycaemia or glucose starvation (Moruno et al., 2012). ROS are produced during OXPHOS via the electron transport chain (ETC) – where a small proportion of molecular oxygen is reduced to superoxide because of a leakage in electrons in the mitochondrial respiratory chain at either complexes I or III (Jastroch et al., 2010).

Initially, ROS were thought to increase proliferation of NSCs and self-renewal of progenitor stem cells, but now appear to display effects that are pleiotropic (Le Belle et al., 2011). In the developing cortex from human hESCs, ROS increases when NSCs differentiate into RGCs and neurons (Khacho et al., 2016). In dopaminergic neurons differentiated over 14 days from hESCs, an upregulation in levels of ROS was identified (Fang et al., 2016). A study found the promotion of differentiation of NSCs by ROS was dependent on NADPH oxidase (NOX2)

activity and not on the mitochondria, and that NOX2 helps maintain proliferation of NSCs via modulation of the Akt/mTOR pathway (Hameed et al., 2015; Le Belle et al., 2011).

High levels or long-term exposure of ROS have shown to decrease mTORC1 activity in vivo and in various cell lines, perhaps via AMPK activation (Hardie et al., 2012) whereas decreased levels of ROS have shown to increase mTORC1 activity (M. Li et al., 2010). However ROS has also been reported to directly oxidize TSC2 leading to its inactivation, causing mTORC1 activation (Yoshida et al., 2011). Furthermore modulators that induce intracellular ROS activate AMPK without an associated decrease in ATP levels (J. Kim et al., 2016). Based on this collective evidence, hyperglycaemia induced ROS is a good candidate to explain the observed relative suppression of mTORC1 in TSC2 KO cells in my study.

Metformin had no meaningful effects on ATP levels in wildtype or TSC2 -/- cells and had complex effects on AMPK activation – capable of reducing or increasing activation. This suggests that the relationship between Metformin and AMPK is more complex than currently considered and may modulate AMPK through pathways independent of ATP. Canonically, metformin inhibits mitochondrial respiratory chain I, leading to a decrease in ATP production and AMPK activation (Hawley et al., 2010). ATP levels have shown to be increased after treatment with metformin in postnatal primary astrocytes and neurons and decreased in the hippocampus (W. Li et al., 2019) highlighting that the cell type may be important. The lack of effect of metformin in my study may relate to different pathways being employed to generate ATP in the early stages of neurogenesis. Oxidative phosphorylation – which is the principal metabolic pathway affected by metformin – may not be a significant source of ATP in neuroepithelial cells.

In low glucose conditions (2.5 mM), metformin has previously been shown to activate the AMPK pathway and supress the proliferation of NSCs (Zang et al., 2009). Metformin has also been shown to stimulate neurogenesis from NSCs via the AMPK-aPKC-CBP pathway (Cao et al., 2022) and can increase expression of MAP2 and Tuj1 via AMPK activation (Ahn & Cho, 2017). My results do not show a simple effect of metformin, with reduction in AMPK activation at Day 6 in wildtype cells and an increase in activation at Day 12. Metformin effects are clearly dependent on the stage of differentiation, and by Day 12, cells may be approaching a neural stem cell like state and hence showing the expected effect on AMPK activation. However, whatever effects metformin is having, it appears to be mediated without significant change in ATP. As previously noted, future studies will need to also evaluate AMP levels to determine if metformin is changing the AMP/ATP ratio. The complex effects of metformin could also be a result of impacts on other pathways. For example, metformin has been shown to reduce inflammation and ER stress induced by high glucose through the inhibition of the caveolin1/AMPKα complex in rat astrocytes (Wang et al., 2021).

In TSC2-/- cells under normogylcaemic conditions, metformin treatment at Day 12, corrected the hyper-activation of AMPK. Despite being able to normalise AMPK activation at Day 12, metformin had no substantial effect on mTOR activation in TSC2 -/- cells in either hyperglycaemic or normoglycaemic conditions. In another study, TSC2 -/- mouse embryonic fibroblasts mTORC1 sensitivity to metformin was dependent on cell confluency (Kalender et al., 2010). This could be examined in the context of neurogenesis in future studies.

Metformin has also been shown to decrease ROS production via inhibition of protein kinase C activity in aortic endothelial and mesenchymal stem cells (Marycz et al., 2016; Ouslimani et

al., 2005). A metformin mediated reduction of ROS levels could therefore plausibly explain the decreased AMPK activity I observed.

Limitations

Quantification of immunofluorescence imaging was not performed. Quantifying these differences in morphology between wildtype and TSC2-/- cells under hyperglycaemic and normoglycaemic conditions could have presented information on how altered glucose supply affects early neurogenesis. Although this study consisted of three biological replicates, increasing patient cell lines may limit biological variability when determining AMPK and mTORC1 activity. Like in most stem-cell based studies, it was crucial to closely monitor the composition of media culture to increase clinical relevancy. As this study illustrated the importance of glucose concentrations, the inclusion of widely used components of media, such as DMEM, in forms without added glucose within said components were utilized for the purpose of improving the accuracy of the glucose supply. By having strict guidelines for media components, it ensured that when glucose is added, there were no unknown contributions to total glucose supply.

Future directions

To further test the effects of altered glucose supply on the stability of metabolic pathways, evaluating ATP levels, AMPK and mTORC1 activity at later timepoints may shed a light on the complex interactions that occur during early neurogenesis. As explored, glucose supply is not the only factor to affect AMPK and mTORC1 activity. Seeing the effects of altered glucose supply without β-mercaptoethanol in media composition can provide more information in the interplay of ROSs as β-mercaptoethanol acts as an antioxidant through scavenging hydroxyl radicals (Petrov et al., 2012). To better understand the effects of Metformin on AMPK activity,

future studies will need to evaluate AMP levels to determine if metformin is affecting the AMP/ATP ratio.

Conclusions

Wildtype cells appear to be stable to altered levels of glucose supply with no significant change in ATP levels or AMPK activity, but a shift in mTORC1 dynamics during early neuronal differentiation. Cells without TSC2 present with dysregulated AMPK in physiological relevant conditions and significantly suppressed mTORC1 activity when cells are in hyperglycaemic conditions. It is clear that TSC2 plays an important role in providing stability of these metabolic pathways during early neurogenesis.

References

Agostini, M., Romeo, F., Inoue, S., Niklison-Chirou, M. V., Elia, A. J., Dinsdale, D., Morone, N., Knight, R. A., Mak, T. W., & Melino, G. (2016). Metabolic reprogramming during neuronal differentiation. *Cell Death & Differentiation*, *23*(9), 1502–1514. https://doi.org/10.1038/cdd.2016.36

Agrawal, P., Reynolds, J., Chew, S., Lamba, D. A., & Hughes, R. E. (2014). DEPTOR Is a Stemness Factor That Regulates Pluripotency of Embryonic Stem Cells. *Journal of Biological Chemistry*, *289*(46), 31818–31826. https://doi.org/10.1074/jbc.M114.565838

Ahn, M., & Cho, G. (2017). Metformin promotes neuronal differentiation and neurite outgrowth through AMPK activation in human bone marrow–mesenchymal stem cells. *Biotechnology and Applied Biochemistry*, *64*(6), 836–842. https://doi.org/10.1002/bab.1584

Amin, S., Lux, A., & O'Callaghan, F. (2019). The journey of metformin from glycaemic control to mTOR inhibition and the suppression of tumour growth. *British Journal of Clinical Pharmacology*, *85*(1), 37–46. https://doi.org/10.1111/bcp.13780

Cao, G., Gong, T., Du, Y., Wang, Y., Ge, T., & Liu, J. (2022). Mechanism of metformin regulation in central nervous system: Progression and future perspectives. *Biomedicine & Pharmacotherapy*, *156*, 113686. https://doi.org/10.1016/j.biopha.2022.113686

Carson, R. P., Van Nielen, D. L., Winzenburger, P. A., & Ess, K. C. (2012). Neuronal and glia abnormalities in Tsc1-deficient forebrain and partial rescue by rapamycin. *Neurobiology of Disease*, *45*(1), 369–380. https://doi.org/10.1016/j.nbd.2011.08.024

Chambers, S. M., Fasano, C. A., Papapetrou, E. P., Tomishima, M., Sadelain, M., & Studer, L. (2009). Highly efficient neural conversion of human ES and iPS cells by dual

inhibition of SMAD signaling. *Nature Biotechnology*, *27*(3), 275–280. https://doi.org/10.1038/nbt.1529

Cloëtta, D., Thomanetz, V., Baranek, C., Lustenberger, R. M., Lin, S., Oliveri, F., Atanasoski, S., & Rüegg, M. A. (2013). Inactivation of mTORC1 in the Developing Brain Causes Microcephaly and Affects Gliogenesis. *The Journal of Neuroscience*, *33*(18), 7799–7810. https://doi.org/10.1523/JNEUROSCI.3294-12.2013

Costa, V., Aigner, S., Vukcevic, M., Sauter, E., Behr, K., Ebeling, M., Dunkley, T., Friedlein, A., Zoffmann, S., Meyer, C. A., Knoflach, F., Lugert, S., Patsch, C., Fjeldskaar, F., Chicha-Gaudimier, L., Kiialainen, A., Piraino, P., Bedoucha, M., Graf, M., … Jagasia, R. (2016). mTORC1 Inhibition Corrects Neurodevelopmental and Synaptic Alterations in a Human Stem Cell Model of Tuberous Sclerosis. *Cell Reports*, *15*(1), 86–95. https://doi.org/10.1016/j.celrep.2016.02.090

Crino, P. B., Nathanson, K. L., & Henske, E. P. (2006). The Tuberous Sclerosis Complex. *New England Journal of Medicine*, *355*(13), 1345–1356. https://doi.org/10.1056/NEJMra055323

Dabora, S. L., Jozwiak, S., Franz, D. N., Roberts, P. S., Nieto, A., Chung, J., Choy, Y.-S., Reeve, M. P., Thiele, E., Egelhoff, J. C., Kasprzyk-Obara, J., Domanska-Pakiela, D., & Kwiatkowski, D. J. (2001). Mutational Analysis in a Cohort of 224 Tuberous Sclerosis Patients Indicates Increased Severity of TSC2, Compared with TSC1, Disease in Multiple Organs. *The American Journal of Human Genetics*, *68*(1), 64–80. https://doi.org/10.1086/316951

Díaz-Alonso, J., Aguado, T., De Salas-Quiroga, A., Ortega, Z., Guzmán, M., & Galve-Roperh, I. (2015). CB $_1$ Cannabinoid Receptor-Dependent Activation of mTORC1/Pax6 Signaling Drives Tbr2 Expression and Basal Progenitor Expansion in

the Developing Mouse Cortex. *Cerebral Cortex*, *25*(9), 2395–2408. https://doi.org/10.1093/cercor/bhu039

Dringen, R., Gebhardt, R., & Hamprecht, B. (1993). Glycogen in astrocytes: Possible function as lactate supply for neighboring cells. *Brain Research*, *623*(2), 208–214. https://doi.org/10.1016/0006-8993(93)91429-V

Easley, C. A., Ben-Yehudah, A., Redinger, C. J., Oliver, S. L., Varum, S. T., Eisinger, V. M., Carlisle, D. L., Donovan, P. J., & Schatten, G. P. (2010). mTOR-Mediated Activation of p70 S6K Induces Differentiation of Pluripotent Human Embryonic Stem Cells. *Cellular Reprogramming*, *12*(3), 263–273. https://doi.org/10.1089/cell.2010.0011

Ebrahimi-Fakhari, D., Saffari, A., Wahlster, L., Di Nardo, A., Turner, D., Lewis, T. L., Conrad, C., Rothberg, J. M., Lipton, J. O., Kölker, S., Hoffmann, G. F., Han, M.-J., Polleux, F., & Sahin, M. (2016). Impaired Mitochondrial Dynamics and Mitophagy in Neuronal Models of Tuberous Sclerosis Complex. *Cell Reports*, *17*(4), 1053–1070. https://doi.org/10.1016/j.celrep.2016.09.054

Fang, D., Qing, Y., Yan, S., Chen, D., & Yan, S. S. (2016). Development and Dynamic Regulation of Mitochondrial Network in Human Midbrain Dopaminergic Neurons Differentiated from iPSCs. *Stem Cell Reports*, *7*(4), 678–692. https://doi.org/10.1016/j.stemcr.2016.08.014

Gal, J. S., Morozov, Y. M., Ayoub, A. E., Chatterjee, M., Rakic, P., & Haydar, T. F. (2006). Molecular and Morphological Heterogeneity of Neural Precursors in the Mouse Neocortical Proliferative Zones. *The Journal of Neuroscience*, *26*(3), 1045–1056. https://doi.org/10.1523/JNEUROSCI.4499-05.2006

Goyal, M. S., Hawrylycz, M., Miller, J. A., Snyder, A. Z., & Raichle, M. E. (2014). Aerobic Glycolysis in the Human Brain Is Associated with Development and Neotenous Gene

Expression. *Cell Metabolism*, *19*(1), 49–57. https://doi.org/10.1016/j.cmet.2013.11.020

Gwinn, D. M., Shackelford, D. B., Egan, D. F., Mihaylova, M. M., Mery, A., Vasquez, D. S., Turk, B. E., & Shaw, R. J. (2008). AMPK Phosphorylation of Raptor Mediates a Metabolic Checkpoint. *Molecular Cell*, *30*(2), 214–226. https://doi.org/10.1016/j.molcel.2008.03.003

Habib, S. L., & Liang, S. (2014). Hyperactivation of Akt/mTOR and deficiency in tuberin increased the oxidative DNA damage in kidney cancer patients with diabetes. *Oncotarget*, *5*(9), 2542–2550. https://doi.org/10.18632/oncotarget.1833

Hahn-Windgassen, A., Nogueira, V., Chen, C.-C., Skeen, J. E., Sonenberg, N., & Hay, N. (2005). Akt Activates the Mammalian Target of Rapamycin by Regulating Cellular ATP Level and AMPK Activity. *Journal of Biological Chemistry*, *280*(37), 32081–32089. https://doi.org/10.1074/jbc.M502876200

Hameed, L. S., Berg, D. A., Belnoue, L., Jensen, L. D., Cao, Y., & Simon, A. (2015). Environmental changes in oxygen tension reveal ROS-dependent neurogenesis and regeneration in the adult newt brain. *eLife*, *4*, e08422. https://doi.org/10.7554/eLife.08422

Hara, K., Maruki, Y., Long, X., Yoshino, K., Oshiro, N., Hidayat, S., Tokunaga, C., Avruch, J., & Yonezawa, K. (2002). Raptor, a Binding Partner of Target of Rapamycin (TOR), Mediates TOR Action. *Cell*, *110*(2), 177–189. https://doi.org/10.1016/S0092-8674(02)00833-4

Hardie, D. G., Ross, F. A., & Hawley, S. A. (2012). AMPK: A nutrient and energy sensor that maintains energy homeostasis. *Nature Reviews Molecular Cell Biology*, *13*(4), 251–262. https://doi.org/10.1038/nrm3311

Hawley, S. A., Ross, F. A., Chevtzoff, C., Green, K. A., Evans, A., Fogarty, S., Towler, M. C., Brown, L. J., Ogunbayo, O. A., Evans, A. M., & Hardie, D. G. (2010). Use of Cells Expressing γ Subunit Variants to Identify Diverse Mechanisms of AMPK Activation. *Cell Metabolism*, *11*(6), 554–565. https://doi.org/10.1016/j.cmet.2010.04.001

Henske, E. P., Jóźwiak, S., Kingswood, J. C., Sampson, J. R., & Thiele, E. A. (2016). Tuberous sclerosis complex. *Nature Reviews Disease Primers*, *2*(1), 16035. https://doi.org/10.1038/nrdp.2016.35

Herrero-Mendez, A., Almeida, A., Fernández, E., Maestre, C., Moncada, S., & Bolaños, J. P. (2009). The bioenergetic and antioxidant status of neurons is controlled by continuous degradation of a key glycolytic enzyme by APC/C–Cdh1. *Nature Cell Biology*, *11*(6), 747–752. https://doi.org/10.1038/ncb1881

Hockemeyer, D., & Jaenisch, R. (2016). Induced Pluripotent Stem Cells Meet Genome Editing. *Cell Stem Cell*, *18*(5), 573–586. https://doi.org/10.1016/j.stem.2016.04.013

Huynh, C., Ryu, J., Lee, J., Inoki, A., & Inoki, K. (2023). Nutrient-sensing mTORC1 and AMPK pathways in chronic kidney diseases. *Nature Reviews Nephrology*, *19*(2), 102–122. https://doi.org/10.1038/s41581-022-00648-y

Inoki, K., Li, Y., Zhu, T., Wu, J., & Guan, K.-L. (2002). TSC2 is phosphorylated and inhibited by Akt and suppresses mTOR signalling. *Nature Cell Biology*, *4*(9), 648–657. https://doi.org/10.1038/ncb839

Ito, K., & Suda, T. (2014). Metabolic requirements for the maintenance of self-renewing stem cells. *Nature Reviews Molecular Cell Biology*, *15*(4), 243–256. https://doi.org/10.1038/nrm3772

Jastroch, M., Divakaruni, A. S., Mookerjee, S., Treberg, J. R., & Brand, M. D. (2010). Mitochondrial proton and electron leaks. *Essays in Biochemistry*, *47*, 53–67. https://doi.org/10.1042/bse0470053

Jinek, M., East, A., Cheng, A., Lin, S., Ma, E., & Doudna, J. (2013). RNA-programmed genome editing in human cells. *eLife*, *2*, e00471. https://doi.org/10.7554/eLife.00471

Jozwiak, J., Jozwiak, S., & Wlodarski, P. (2008). Possible mechanisms of disease development in tuberous sclerosis. *The Lancet Oncology*, *9*(1), 73–79. https://doi.org/10.1016/S1470-2045(07)70411-4

Kalender, A., Selvaraj, A., Kim, S. Y., Gulati, P., Brûlé, S., Viollet, B., Kemp, B. E., Bardeesy, N., Dennis, P., Schlager, J. J., Marette, A., Kozma, S. C., & Thomas, G. (2010). Metformin, Independent of AMPK, Inhibits mTORC1 in a Rag GTPase-Dependent Manner. *Cell Metabolism*, *11*(5), 390–401. https://doi.org/10.1016/j.cmet.2010.03.014

Khacho, M., Clark, A., Svoboda, D. S., Azzi, J., MacLaurin, J. G., Meghaizel, C., Sesaki, H., Lagace, D. C., Germain, M., Harper, M.-E., Park, D. S., & Slack, R. S. (2016). Mitochondrial Dynamics Impacts Stem Cell Identity and Fate Decisions by Regulating a Nuclear Transcriptional Program. *Cell Stem Cell*, *19*(2), 232–247. https://doi.org/10.1016/j.stem.2016.04.015

Kim, D.-H., Sarbassov, D. D., Ali, S. M., King, J. E., Latek, R. R., Erdjument-Bromage, H., Tempst, P., & Sabatini, D. M. (2002). mTOR Interacts with Raptor to Form a Nutrient-Sensitive Complex that Signals to the Cell Growth Machinery. *Cell*, *110*(2), 163–175. https://doi.org/10.1016/S0092-8674(02)00808-5

Kim, J., Yang, G., Kim, Y., Kim, J., & Ha, J. (2016). AMPK activators: Mechanisms of action and physiological activities. *Experimental & Molecular Medicine*, *48*(4), e224–e224. https://doi.org/10.1038/emm.2016.16

Kondoh, H., Lleonart, M. E., Nakashima, Y., Yokode, M., Tanaka, M., Bernard, D., Gil, J., & Beach, D. (2007). A High Glycolytic Flux Supports the Proliferative Potential of Murine Embryonic Stem Cells. *Antioxidants & Redox Signaling*, *9*(3), 293–299. https://doi.org/10.1089/ars.2006.1467

Le Belle, J. E., Orozco, N. M., Paucar, A. A., Saxe, J. P., Mottahedeh, J., Pyle, A. D., Wu, H., & Kornblum, H. I. (2011). Proliferative Neural Stem Cells Have High Endogenous ROS Levels that Regulate Self-Renewal and Neurogenesis in a PI3K/Akt-Dependant Manner. *Cell Stem Cell*, *8*(1), 59–71. https://doi.org/10.1016/j.stem.2010.11.028

Lee, H.-K., Lee, H.-S., & Moody, S. A. (2014). Neural Transcription Factors: From Embryos to Neural Stem Cells. *Molecules and Cells*, *37*(10), 705–712. https://doi.org/10.14348/molcells.2014.0227

Li, M., Zhao, L., Liu, J., Liu, A., Jia, C., Ma, D., Jiang, Y., & Bai, X. (2010). Multi-mechanisms are involved in reactive oxygen species regulation of mTORC1 signaling. *Cellular Signalling*, *22*(10), 1469–1476. https://doi.org/10.1016/j.cellsig.2010.05.015

Li, W., Chaudhari, K., Shetty, R., Winters, A., Gao, X., Hu, Z., Ge, W.-P., Sumien, N., Forster, M., Liu, R., & Yang, S.-H. (2019). Metformin Alters Locomotor and Cognitive Function and Brain Metabolism in Normoglycemic Mice. *Aging and Disease*, *10*(5), 949. https://doi.org/10.14336/AD.2019.0120

LiCausi, F., & Hartman, N. (2018). Role of mTOR Complexes in Neurogenesis. *International Journal of Molecular Sciences*, *19*(5), 1544. https://doi.org/10.3390/ijms19051544

Lunt, S. Y., & Vander Heiden, M. G. (2011). Aerobic Glycolysis: Meeting the Metabolic Requirements of Cell Proliferation. *Annual Review of Cell and Developmental Biology*, *27*(1), 441–464. https://doi.org/10.1146/annurev-cellbio-092910-154237

Maffezzini, C., Calvo-Garrido, J., Wredenberg, A., & Freyer, C. (2020). Metabolic regulation of neurodifferentiation in the adult brain. *Cellular and Molecular Life Sciences*, *77*(13), 2483–2496. https://doi.org/10.1007/s00018-019-03430-9

Magri, L., Cambiaghi, M., Cominelli, M., Alfaro-Cervello, C., Cursi, M., Pala, M., Bulfone, A., Garcìa-Verdugo, J. M., Leocani, L., Minicucci, F., Poliani, P. L., & Galli, R. (2011). Sustained Activation of mTOR Pathway in Embryonic Neural Stem Cells Leads to Development of Tuberous Sclerosis Complex-Associated Lesions. *Cell Stem Cell*, *9*(5), 447–462. https://doi.org/10.1016/j.stem.2011.09.008

Marycz, K., Tomaszewski, K. A., Kornicka, K., Henry, B. M., Wroński, S., Tarasiuk, J., & Maredziak, M. (2016). Metformin Decreases Reactive Oxygen Species, Enhances Osteogenic Properties of Adipose-Derived Multipotent Mesenchymal Stem Cells *In Vitro* , and Increases Bone Density *In Vivo*. *Oxidative Medicine and Cellular Longevity*, *2016*, 1–19. https://doi.org/10.1155/2016/9785890

Mihaylova, M. M., & Shaw, R. J. (2011). The AMPK signalling pathway coordinates cell growth, autophagy and metabolism. *Nature Cell Biology*, *13*(9), 1016–1023. https://doi.org/10.1038/ncb2329

Mira, H., & Morante, J. (2020). Neurogenesis From Embryo to Adult – Lessons From Flies and Mice. *Frontiers in Cell and Developmental Biology*, *8*, 533. https://doi.org/10.3389/fcell.2020.00533

Mitchell, P. (1961). Coupling of Phosphorylation to Electron and Hydrogen Transfer by a Chemi-Osmotic type of Mechanism. *Nature*, *191*(4784), 144–148. https://doi.org/10.1038/191144a0

Moruno, F., Pérez-Jiménez, E., & Knecht, E. (2012). Regulation of Autophagy by Glucose in Mammalian Cells. *Cells*, *1*(3), 372–395. https://doi.org/10.3390/cells1030372

Mukhtar, T., & Taylor, V. (2018). Untangling Cortical Complexity During Development. *Journal of Experimental Neuroscience*, *12*, 117906951875933. https://doi.org/10.1177/1179069518759332

Naseh, N., Canto Moreira, N., Vaz, T. F., Gonzalez Tamez, K., Ferreira, H., Kaul, Y. F., Johansson, M., Diderholm, B., Ahlsson, F., Ågren, J., & Hellström-Westas, L. (2022). Early Hyperglycemia in Very Preterm Infants Is Associated with Reduced White Matter Volume and Worse Cognitive and Motor Outcomes at 2.5 Years. *Neonatology*, *119*(6), 745–752. https://doi.org/10.1159/000524923

Nojima, H., Tokunaga, C., Eguchi, S., Oshiro, N., Hidayat, S., Yoshino, K., Hara, K., Tanaka, N., Avruch, J., & Yonezawa, K. (2003). The Mammalian Target of Rapamycin (mTOR) Partner, Raptor, Binds the mTOR Substrates p70 S6 Kinase and 4E-BP1 through Their TOR Signaling (TOS) Motif. *Journal of Biological Chemistry*, *278*(18), 15461–15464. https://doi.org/10.1074/jbc.C200665200

Oakhill, J. S., Steel, R., Chen, Z.-P., Scott, J. W., Ling, N., Tam, S., & Kemp, B. E. (2011). AMPK Is a Direct Adenylate Charge-Regulated Protein Kinase. *Science*, *332*(6036), 1433–1435. https://doi.org/10.1126/science.1200094

Ouslimani, N., Peynet, J., Bonnefont-Rousselot, D., Thérond, P., Legrand, A., & Beaudeux, J.-L. (2005). Metformin decreases intracellular production of reactive oxygen species in aortic endothelial cells. *Metabolism*, *54*(6), 829–834. https://doi.org/10.1016/j.metabol.2005.01.029

Paridaen, J. T., & Huttner, W. B. (2014). Neurogenesis during development of the vertebrate central nervous system. *EMBO Reports*, *15*(4), 351–364. https://doi.org/10.1002/embr.201438447

Pernas, L., & Scorrano, L. (2016). Mito-Morphosis: Mitochondrial Fusion, Fission, and Cristae Remodeling as Key Mediators of Cellular Function. *Annual Review of Physiology*, *78*(1), 505–531. https://doi.org/10.1146/annurev-physiol-021115-105011

Petrov, L., Atanassova, M., & Alexandrova, A. (2012). Comparative study of the antioxidant activity of some thiol-containing substances. *Open Medicine*, *7*(2), 269–273. https://doi.org/10.2478/s11536-011-0132-z

Richter, E. A., & Ruderman, N. B. (2009). AMPK and the biochemistry of exercise: Implications for human health and disease. *Biochemical Journal*, *418*(2), 261–275. https://doi.org/10.1042/BJ20082055

Ritter, S. (2017). Monitoring and Maintenance of Brain Glucose Supply. In R. B. S. Harris (Ed.), *Appetite and Food Intake* (2nd ed., pp. 177–204). CRC Press. https://doi.org/10.1201/9781315120171-9

Rocktäschel, P., Sen, A., & Cader, M. Z. (2019). High glucose concentrations mask cellular phenotypes in a stem cell model of tuberous sclerosis complex. *Epilepsy & Behavior*, *101*, 106581. https://doi.org/10.1016/j.yebeh.2019.106581

Russo, V. C., Higgins, S., Werther, G. A., & Cameron, F. J. (2012). Effects of Fluctuating Glucose Levels on Neuronal Cells In Vitro. *Neurochemical Research*, *37*(8), 1768–1782. https://doi.org/10.1007/s11064-012-0789-y

Sarbassov, D. D., Ali, S. M., & Sabatini, D. M. (2005). Growing roles for the mTOR pathway. *Current Opinion in Cell Biology*, *17*(6), 596–603. https://doi.org/10.1016/j.ceb.2005.09.009

Schurr, A. (2018). Glycolysis Paradigm Shift Dictates a Reevaluation of Glucose and Oxygen Metabolic Rates of Activated Neural Tissue. *Frontiers in Neuroscience*, *12*, 700. https://doi.org/10.3389/fnins.2018.00700

Shaw, R. J., Kosmatka, M., Bardeesy, N., Hurley, R. L., Witters, L. A., DePinho, R. A., & Cantley, L. C. (2004). The tumor suppressor LKB1 kinase directly activates AMP-activated kinase and regulates apoptosis in response to energy stress. *Proceedings of the National Academy of Sciences*, *101*(10), 3329–3335. https://doi.org/10.1073/pnas.0308061100

Shi, Y., Kirwan, P., & Livesey, F. J. (2012). Directed differentiation of human pluripotent stem cells to cerebral cortex neurons and neural networks. *Nature Protocols*, *7*(10), 1836–1846. https://doi.org/10.1038/nprot.2012.116

Shin, J., Berg, D. A., Zhu, Y., Shin, J. Y., Song, J., Bonaguidi, M. A., Enikolopov, G., Nauen, D. W., Christian, K. M., Ming, G., & Song, H. (2015). Single-Cell RNA-Seq with Waterfall Reveals Molecular Cascades underlying Adult Neurogenesis. *Cell Stem Cell*, *17*(3), 360–372. https://doi.org/10.1016/j.stem.2015.07.013

Soldner, F., & Jaenisch, R. (2018). Stem Cells, Genome Editing, and the Path to Translational Medicine. *Cell*, *175*(3), 615–632. https://doi.org/10.1016/j.cell.2018.09.010

Stanescu, A., & Stoicescu, S. M. (2014). Neonatal hypoglycemia screening in newborns from diabetic mothers—Arguments and controversies. *Journal of Medicine and Life*, *7 Spec No. 3*(Spec Iss 3), 51–52.

Suzuki, S., Namiki, J., Shibata, S., Mastuzaki, Y., & Okano, H. (2010). The Neural Stem/Progenitor Cell Marker Nestin Is Expressed in Proliferative Endothelial Cells, but Not in Mature Vasculature. *Journal of Histochemistry & Cytochemistry*, *58*(8), 721–730. https://doi.org/10.1369/jhc.2010.955609

Takubo, K., Nagamatsu, G., Kobayashi, C. I., Nakamura-Ishizu, A., Kobayashi, H., Ikeda, E., Goda, N., Rahimi, Y., Johnson, R. S., Soga, T., Hirao, A., Suematsu, M., & Suda, T. (2013). Regulation of Glycolysis by Pdk Functions as a Metabolic Checkpoint for

Cell Cycle Quiescence in Hematopoietic Stem Cells. *Cell Stem Cell*, *12*(1), 49–61. https://doi.org/10.1016/j.stem.2012.10.011

Tam, P. P. L., & Loebel, D. A. F. (2007). Gene function in mouse embryogenesis: Get set for gastrulation. *Nature Reviews Genetics*, *8*(5), 368–381. https://doi.org/10.1038/nrg2084

Vadodaria, K. C., Jones, J. R., Linker, S., & Gage, F. H. (2020). Modeling Brain Disorders Using Induced Pluripotent Stem Cells. *Cold Spring Harbor Perspectives in Biology*, *12*(6), a035659. https://doi.org/10.1101/cshperspect.a035659

Wang, G., Cui, W., Chen, S., Shao, Z., Li, Y., Wang, W., Mao, L., Li, J., & Mei, X. (2021). Metformin alleviates high glucose-induced ER stress and inflammation by inhibiting the interaction between caveolin1 and AMPKα in rat astrocytes. *Biochemical and Biophysical Research Communications*, *534*, 908–913. https://doi.org/10.1016/j.bbrc.2020.10.075

Watanabe, R., Tambe, Y., Inoue, H., Isono, T., Haneda, M., Isobe, K., Kobayashi, T., Hino, O., Okabe, H., & Chano, T. (2007). GADD34 inhibits mammalian target of rapamycin signaling via tuberous sclerosis complex and controls cell survival under bioenergetic stress. *International Journal of Molecular Medicine*. https://doi.org/10.3892/ijmm.19.3.475

Wong, M. (2019). The role of glia in epilepsy, intellectual disability, and other neurodevelopmental disorders in tuberous sclerosis complex. *Journal of Neurodevelopmental Disorders*, *11*(1), 30. https://doi.org/10.1186/s11689-019-9289-6

Woodbury, M. E., & Ikezu, T. (2014). Fibroblast Growth Factor-2 Signaling in Neurogenesis and Neurodegeneration. *Journal of Neuroimmune Pharmacology*, *9*(2), 92–101. https://doi.org/10.1007/s11481-013-9501-5

Xiao, B., Sanders, M. J., Underwood, E., Heath, R., Mayer, F. V., Carmena, D., Jing, C., Walker, P. A., Eccleston, J. F., Haire, L. F., Saiu, P., Howell, S. A., Aasland, R., Martin, S. R., Carling, D., & Gamblin, S. J. (2011). Structure of mammalian AMPK and its regulation by ADP. *Nature*, *472*(7342), 230–233. https://doi.org/10.1038/nature09932

Yoshida, S., Hong, S., Suzuki, T., Nada, S., Mannan, A. M., Wang, J., Okada, M., Guan, K.-L., & Inoki, K. (2011). Redox regulates mammalian target of rapamycin complex 1 (mTORC1) activity by modulating the TSC1/TSC2-Rheb GTPase pathway. *The Journal of Biological Chemistry*, *286*(37), 32651–32660. https://doi.org/10.1074/jbc.M111.238014

Zang, Y., Yu, L.-F., Nan, F.-J., Feng, L.-Y., & Li, J. (2009). AMP-activated Protein Kinase Is Involved in Neural Stem Cell Growth Suppression and Cell Cycle Arrest by 5-Aminoimidazole-4-carboxamide-1-β-d-ribofuranoside and Glucose Deprivation by Down-regulating Phospho-retinoblastoma Protein and Cyclin D. *Journal of Biological Chemistry*, *284*(10), 6175–6184. https://doi.org/10.1074/jbc.M806887200

Zhang, J., Khvorostov, I., Hong, J. S., Oktay, Y., Vergnes, L., Nuebel, E., Wahjudi, P. N., Setoguchi, K., Wang, G., Do, A., Jung, H.-J., McCaffery, J. M., Kurland, I. J., Reue, K., Lee, W.-N. P., Koehler, C. M., & Teitell, M. A. (2011). UCP2 regulates energy metabolism and differentiation potential of human pluripotent stem cells: UCP2 regulates hPSC metabolism and differentiation. *The EMBO Journal*, *30*(24), 4860–4873. https://doi.org/10.1038/emboj.2011.401

Zhang, X., Huang, C. T., Chen, J., Pankratz, M. T., Xi, J., Li, J., Yang, Y., LaVaute, T. M., Li, X.-J., Ayala, M., Bondarenko, G. I., Du, Z.-W., Jin, Y., Golos, T. G., & Zhang, S.-C. (2010). Pax6 Is a Human Neuroectoderm Cell Fate Determinant. *Cell Stem Cell*, *7*(1), 90–100. https://doi.org/10.1016/j.stem.2010.04.017

Zheng, X., Boyer, L., Jin, M., Mertens, J., Kim, Y., Ma, L., Ma, L., Hamm, M., Gage, F. H., & Hunter, T. (2016). Metabolic reprogramming during neuronal differentiation from aerobic glycolysis to neuronal oxidative phosphorylation. *eLife*, *5*, e13374. https://doi.org/10.7554/eLife.13374

Zheng, Y., Luo, A., & Liu, X. (2021). The Imbalance of Mitochondrial Fusion/Fission Drives High-Glucose-Induced Vascular Injury. *Biomolecules*, *11*(12), 1779. https://doi.org/10.3390/biom11121779

Zhou, W., Zhao, T., Du, J., Ji, G., Li, X., Ji, S., Tian, W., Wang, X., & Hao, A. (2019). TIGAR promotes neural stem cell differentiation through acetyl-CoA-mediated histone acetylation. *Cell Death & Disease*, *10*(3), 198. https://doi.org/10.1038/s41419-019-1434-3

Appendix:

Table 1. Cell culture components and concentrations

Components	Final Conc.
DMEM no glucose (Gibco 11966)	1:1
Neurobasal no glucose (Gibco A2477501)	
50X B27 (Gibco 17504-044)	1%
100X N2 (Gibco 17502-048)	0.5%
50mM β-mercaptoethanol (Gibco 31350-010)	50 µM
100X Glutamax-I (200mM) (Gibco 35050-038)	1mM
10,000 U/ml Penicillin–streptomycin (Gibco 15140122)	25 U/ml
10 mg/mL Insulin (Sigma I9278)	2.5 µg/ml
100mM Sodium pyruvate (Gibco 11360070)	0.5 mM
100X MEM NEAA (10mM) (11140-035)	50 µM
1.1 M (200 g/l) D-Glucose (A2494001)	25mM or 5mM

Table 2. List of primer sequences

Target	Forward Primer (5'-3')	Reverse Primer (5'-3')
GAPDH	GTCTCCTCTGACTTCAACAGCG	ACCACCCTGTTGCTGTAGCCAA
PAX6	GTGTCCAACGGATGTGTGAG	CTAGCCAGGTTGCGAAGAAC
Nestin	CTCAGCTTTCAGGACCCCAA	GTCTCAAGGGTAGCAGGCAA
Oct4	TCGAGAACCGAGTGAGAGG	GAACCACACTCGGACCACA
Nanog	AGCGAATCTTCACCAATGCC	TGCTTCTTGACTGGGACCTT
Sox2	TTACCTCTTCCTCCCACTCCAG	GGGTTTTCTCCATGCTGTTTCT
TSC2	GAGAGGAGCCGTGTTTTTTGTG	GACATGCCATGGCCTGGTA
bActin	CATGTACGTTGCTATCCAGGC	CTCCTTAATGTCACGCACGAT

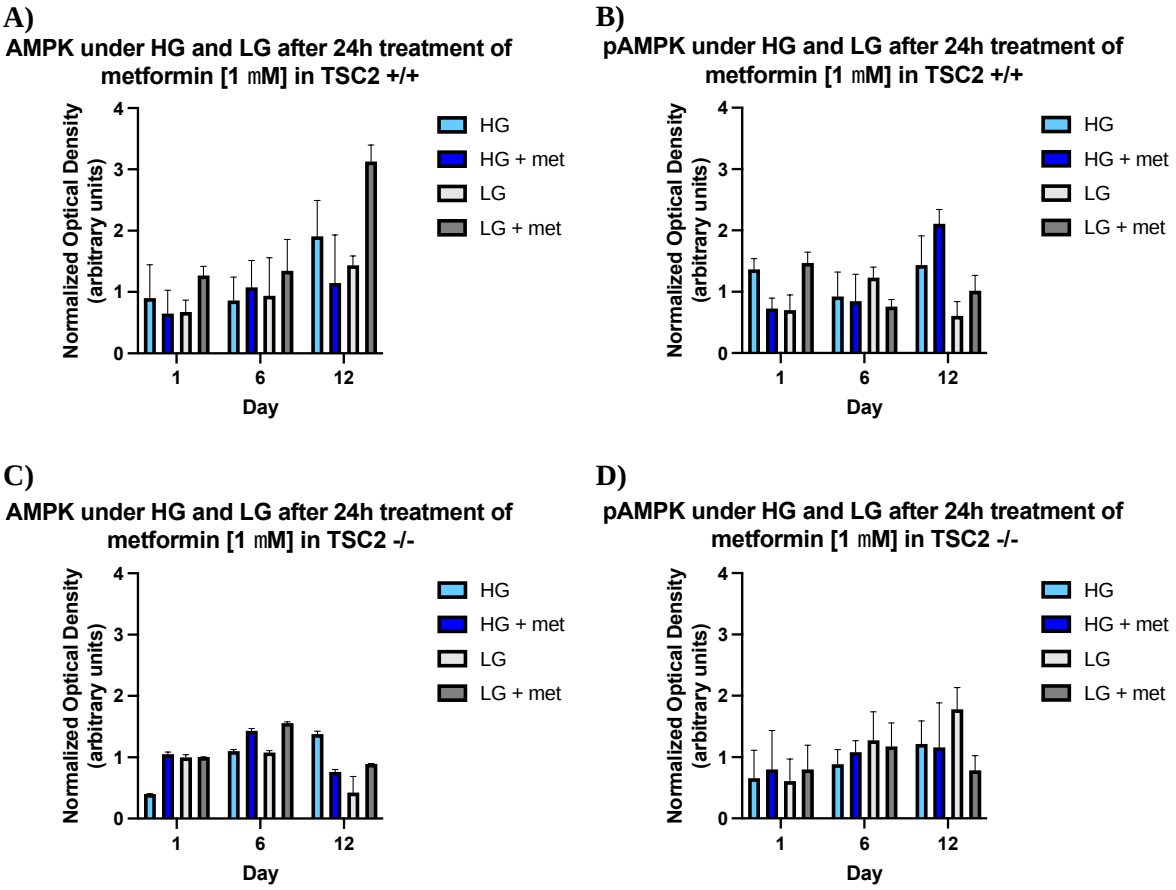

Figure 9: Normalized Optical Density of AMPK and pAMPK used for pAMPK/AMPK in isogenic control and TSC2 -/-.

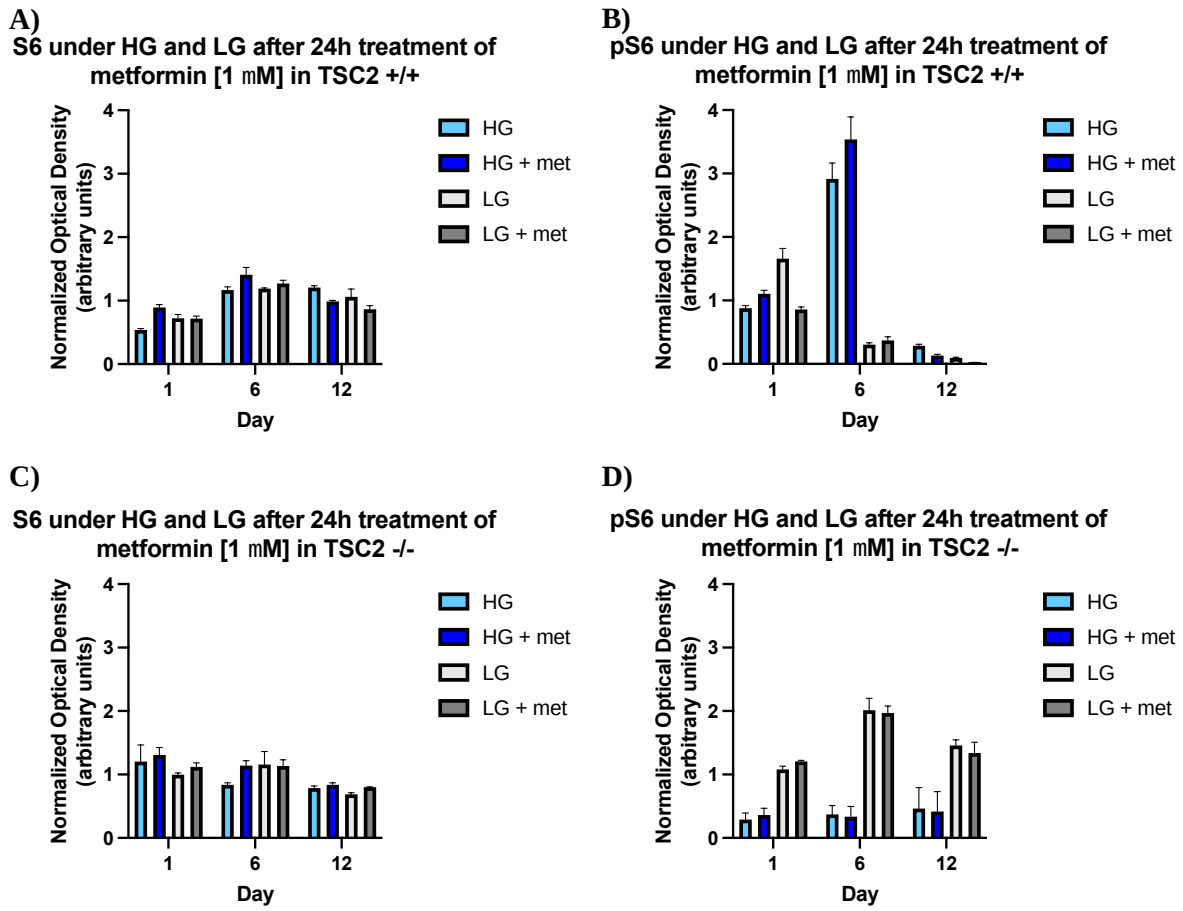

Figure 10: Normalized Optical Density of S6 and pS6 used for pS6/S6 in isogenic control and TSC2 -/-.

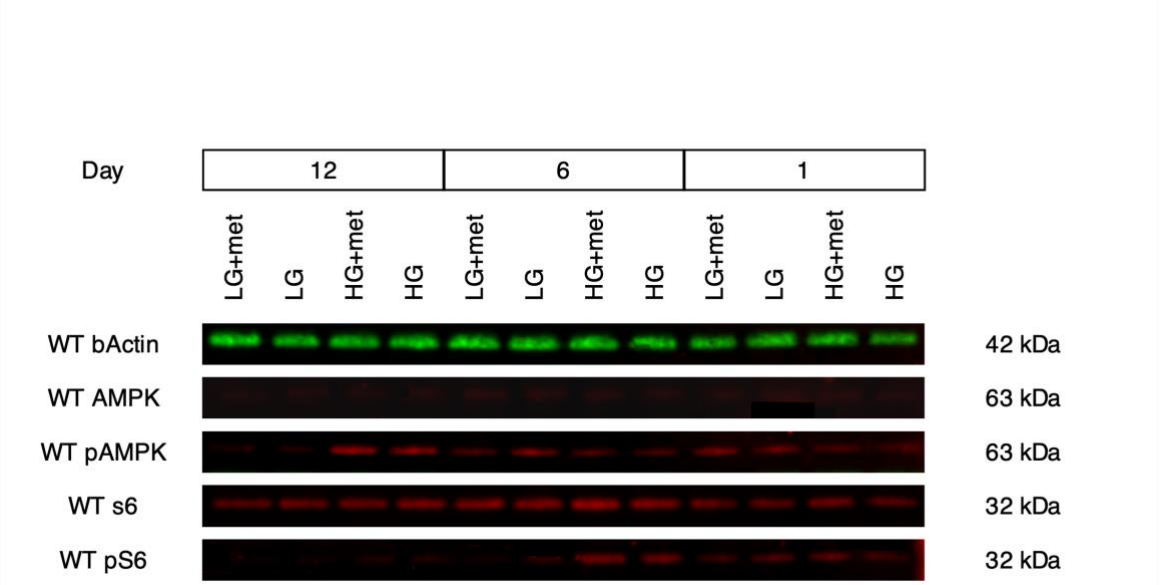

Figure 11: Protein expression pattern of bActin, AMPK, pAMPK, S6 and pS6 in isogenic control (TSC2 +/+).

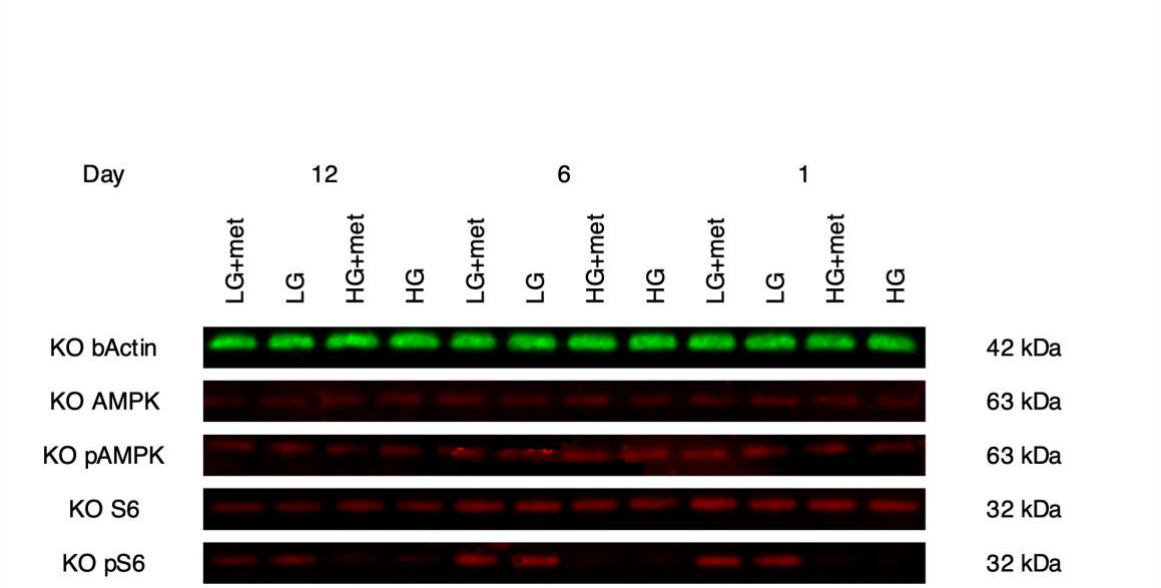

Figure 12: Protein expression pattern of bActin, AMPK, pAMPK, S6 and pS6 in TSC2 -/-.